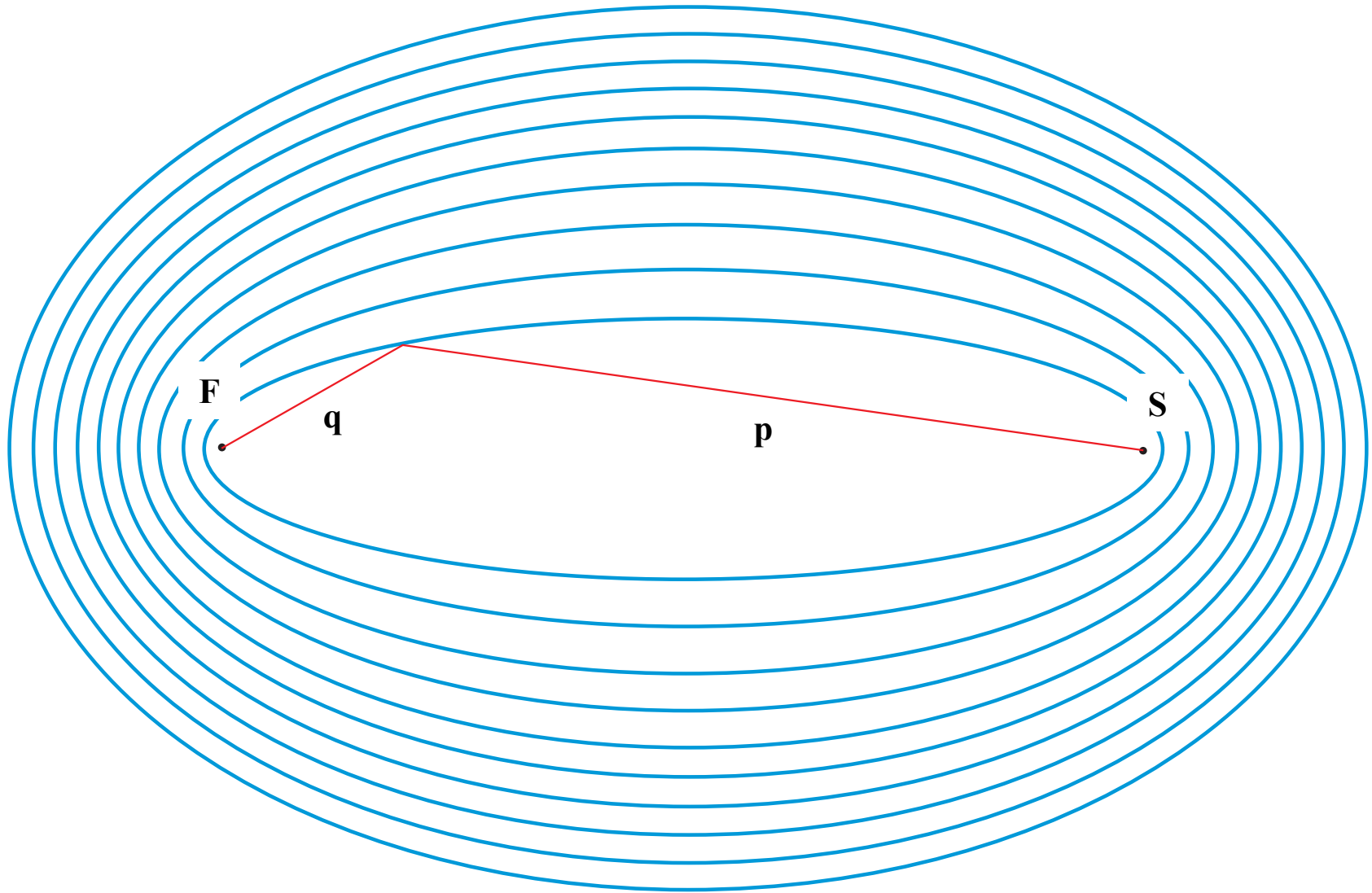


Mirror and multilayer x-ray optics

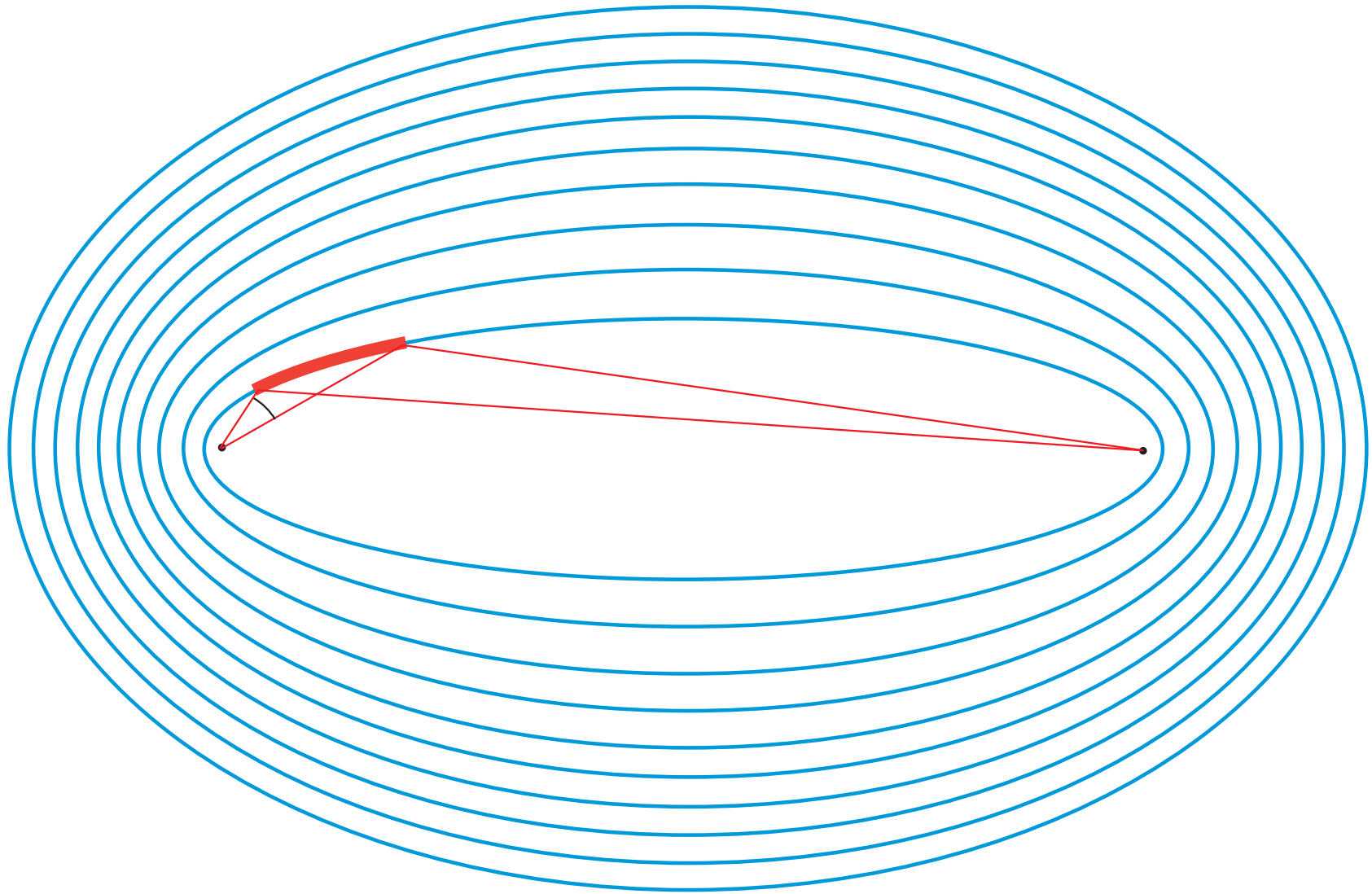
Ch. Morawe, ESRF Optics Group

- Background and theory
- Design, fabrication, and characterization
- Performance and limitations
- Applications
- Summary and perspectives

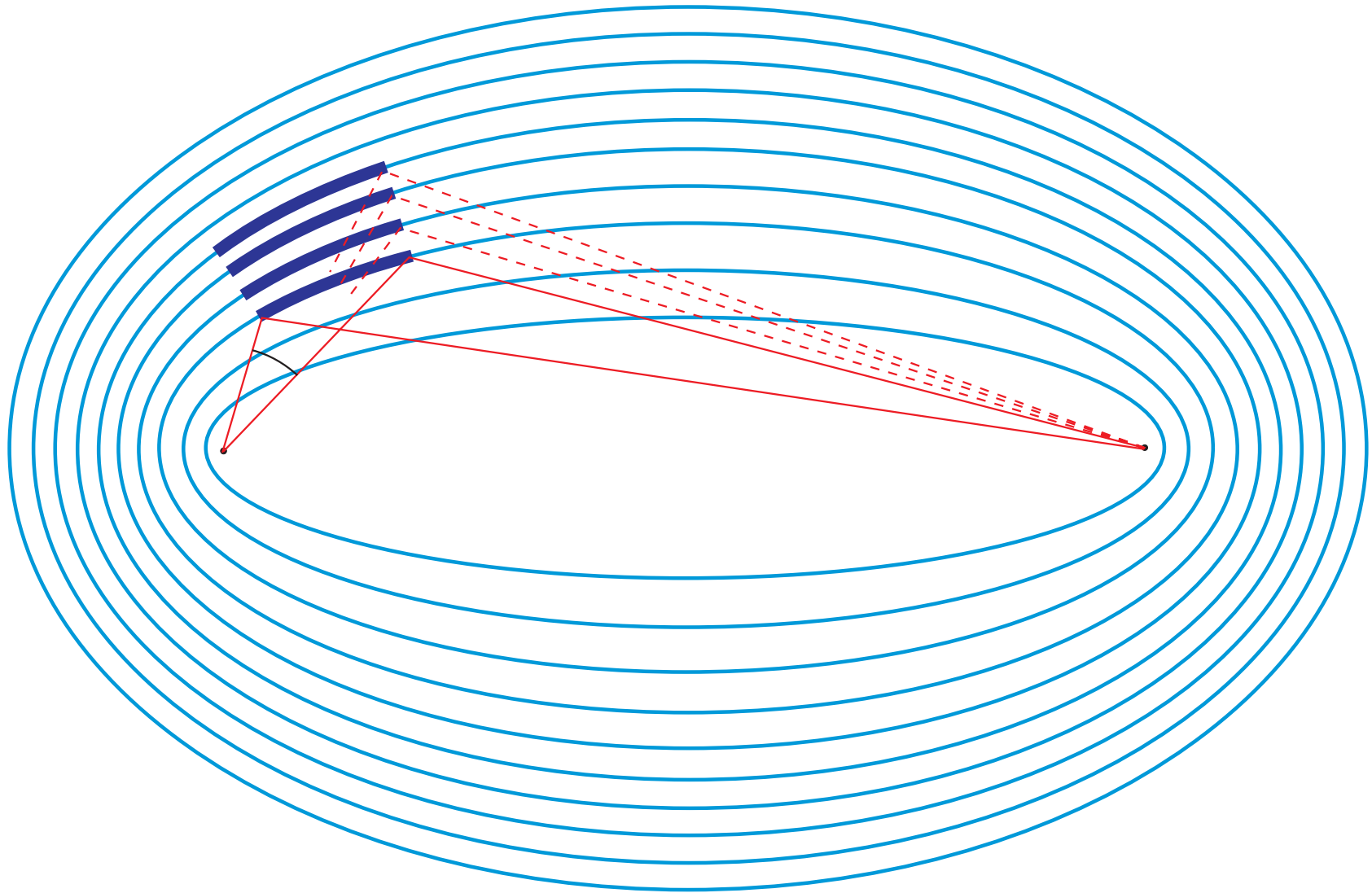
Basic geometry



Mirror optics



Multilayer optics



Interaction of x-rays with matter

Elastic (Thompson) scattering by a free electron

$$\sigma_{el} = \frac{8\pi}{3} \cdot r_e^2$$

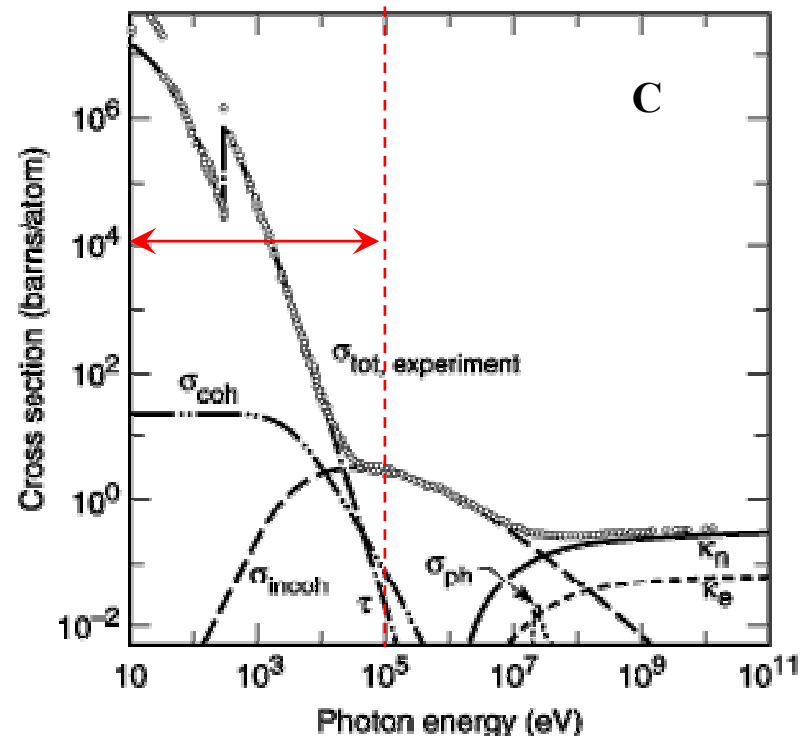
Coherent/elastic (Rayleigh) scattering from atoms

$$\sigma_{coh} = \pi \cdot r_e^2 \int_{-1}^{+1} |f(\theta)|^2 \cdot (1 + \cos^2 \theta) \cdot d(\cos \theta)$$

Total cross section

$$\sigma_{tot} = \sigma_{coh} + \tau + \sigma_{incoh} + \sigma_{ph} + \kappa_n + \kappa_e$$

- σ_{coh} : Coherent elastic scattering
- τ : Atomic photo effect
- σ_{incoh} : Compton scattering
- σ_{ph} : Nuclear absorption
- κ_i : Pair production



[1] J.H. Hubbel et al, J. Phys. Chem. Ref. Data 9, 1023 (1980)

Interaction of x-rays with matter

Definition of optical index for x-rays ($E > 30\text{eV}$)

Atomic form factor

$$f(\vec{q}, E) = f_0(\vec{q}) + f_1(E) + if_2(E)$$

free electrons bound electrons absorption

Atomic cross section → Optical index n

Comparison between refraction and scattering description [2]

$$n = 1 - \delta + i\beta \quad e^{inkz} = e^{i(1-\delta)kz} \cdot e^{-\beta kz} \quad \delta = \frac{2\pi\rho_a r_e}{k^2} (f_0 + f_1) \quad \beta = \frac{4\pi\rho_a r_e}{2k^2} f_2$$

In terms of total atomic scattering factor

$$n = 1 - \frac{2\pi\rho_a r_e}{k^2} [f_0(\vec{q}) + f_1(E) + if_2(E)]$$

$$k = \frac{2\pi}{\lambda}$$

Typical value: **n ~ 1 - 10⁻⁵ @ 10 keV** < 1 !

Interaction of x-rays with matter

Practical aspects

Vast compilation of atomic scattering data e.g. by CXRO – ALS Berkeley (USA)

Data booklet and web site <http://www-cxro.lbl.gov> [3] – [4]

Dedicated area of research (theory and experiment)

VUV – EUV – Soft x-ray range:

Optical index very complex (many electronic states and transitions) and still under investigation

Hard x-rays:

Optical index well known and documented

Interaction of x-rays with matter

Experimental data

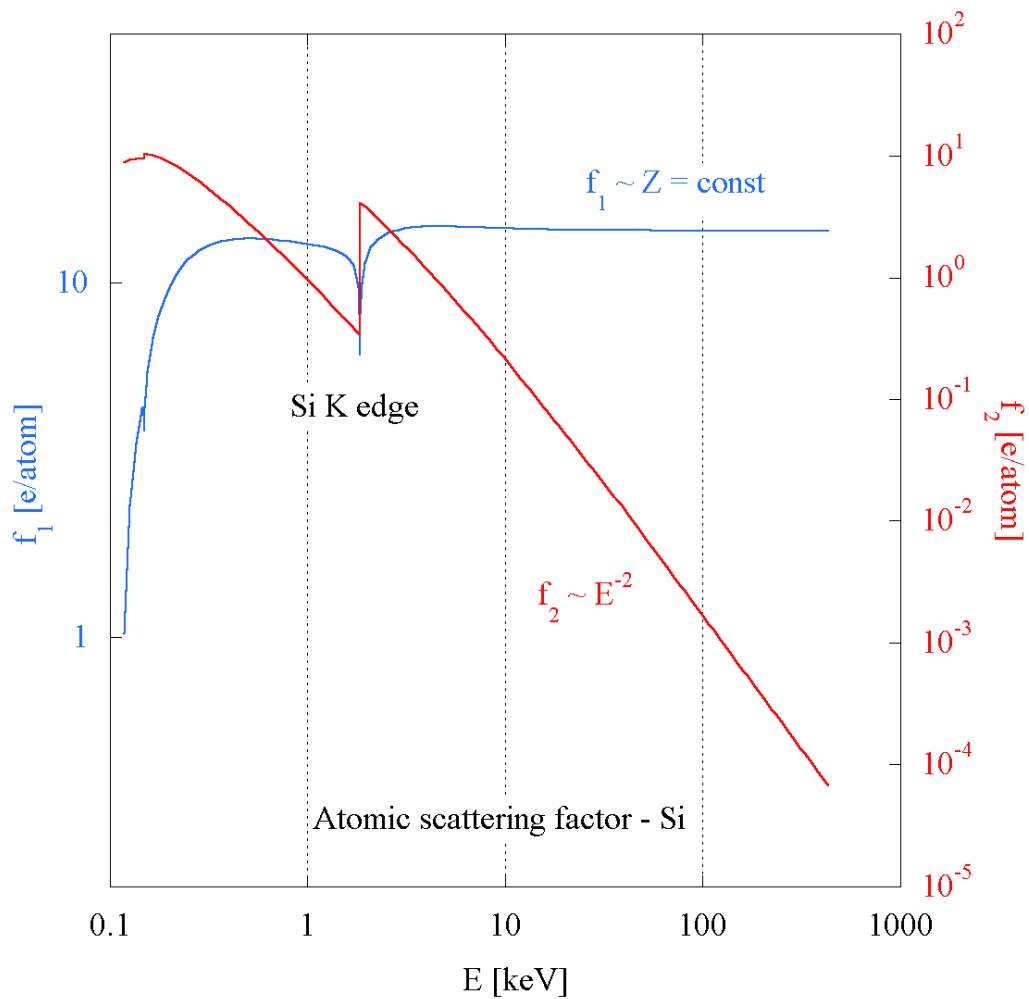
Asymptotic behaviour for $E > E(K)$:

$$f_1 \approx \text{const} \quad f_2 \approx 1/E^2$$

$$\delta \approx 1/E^2 \quad \beta \approx 1/E^4$$

$$\frac{\delta}{\beta} \approx E^2$$

High energy applications !



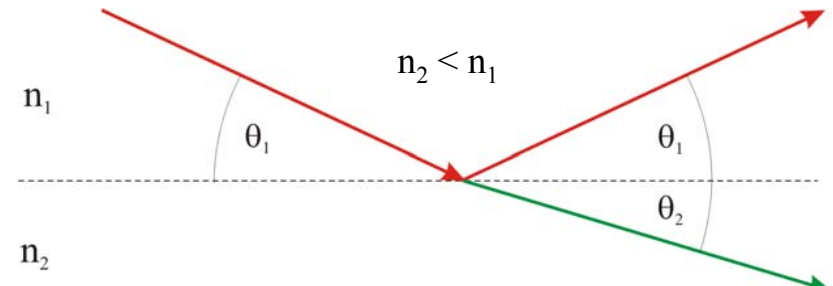
Reflection and refraction

Snell's law

$$\frac{n_1}{n_2} = \frac{\cos \theta_2}{\cos \theta_1}$$

Total reflection for $\theta_1 < \theta_C$

$$\cos \theta_C = \frac{n_2}{n_1}$$



Typical value: $\theta_C \sim 5 \text{ mrad} \sim 0.3^\circ @ 10 \text{ keV}$

Wave propagation along interface, damped amplitude normal to it
No energy flux across interface!

Total reflection x-ray mirrors !

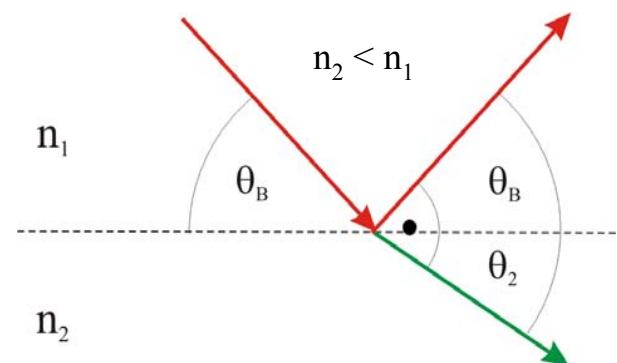
Polarization

$$E_\pi = 0 \Leftrightarrow \theta_1 + \theta_2 = 90^\circ$$

Brewster angle

$$\tan(\theta_B) = \frac{n_1}{n_2}$$

Soft x-ray multilayer polarizers !



Reflection and refraction

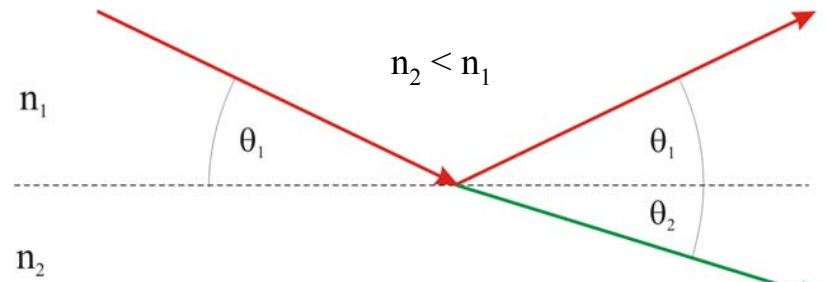
Fresnel formulae for reflection and transmission amplitudes

$$r_\sigma = \frac{n_1 \sin \theta_1 - n_2 \sin \theta_2}{n_1 \sin \theta_1 + n_2 \sin \theta_2}$$

$$r_\pi = \frac{n_1 \sin \theta_2 - n_2 \sin \theta_1}{n_1 \sin \theta_2 + n_2 \sin \theta_1}$$

$$t_\sigma = \frac{2n_1 \sin \theta_1}{n_1 \sin \theta_1 + n_2 \sin \theta_2}$$

$$t_\pi = \frac{2n_1 \sin \theta_2}{n_1 \sin \theta_2 + n_2 \sin \theta_1}$$



Reflectivity amplitude as a function of external angle of incidence θ (vacuum)

$$r_\sigma = \frac{\sqrt{n_1^2 - \cos^2 \theta} - \sqrt{n_2^2 - \cos^2 \theta}}{\sqrt{n_1^2 - \cos^2 \theta} + \sqrt{n_2^2 - \cos^2 \theta}}$$

$$r_\pi = \frac{n_1/n_2 \sqrt{n_2^2 - \cos^2 \theta} - n_2/n_1 \sqrt{n_1^2 - \cos^2 \theta}}{n_1/n_2 \sqrt{n_2^2 - \cos^2 \theta} + n_2/n_1 \sqrt{n_1^2 - \cos^2 \theta}}$$

Including graded interfaces (Gaussian density gradient, phase shift)

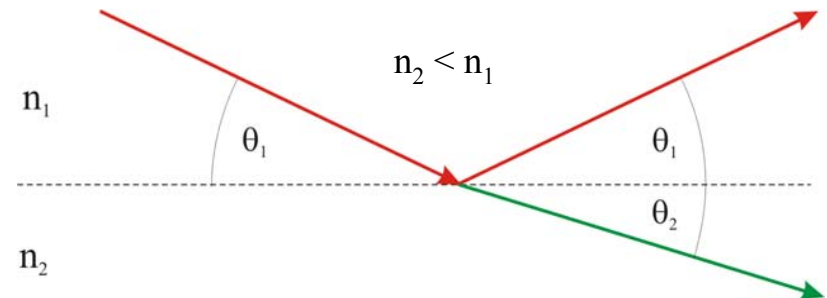
$$r = r_{ideal} \cdot e^{-\frac{8\pi^2}{\lambda^2} \sqrt{n_1^2 - \cos^2 \theta} \sqrt{n_2^2 - \cos^2 \theta} \sigma^2}$$

Reflection and refraction

Reflected and transmitted intensity

$$R = \frac{-\Phi_{ref}}{\Phi_{in}} = \frac{k_1 \cdot \sin \theta_1 \cdot |r|^2}{k_1 \cdot \sin \theta_1 \cdot |l|} = |r|^2$$

$$T = \frac{\Phi_{trans}}{\Phi_{in}} = \frac{k_2 \cdot \sin \theta_2 \cdot |t|^2}{k_1 \cdot \sin \theta_1 \cdot |l|} = \frac{n_2 \cdot \sin \theta_2}{n_1 \cdot \sin \theta_1} |t|^2$$



Graded interface: Lower reflectivity but enhanced transmission

See also [5] – [7]

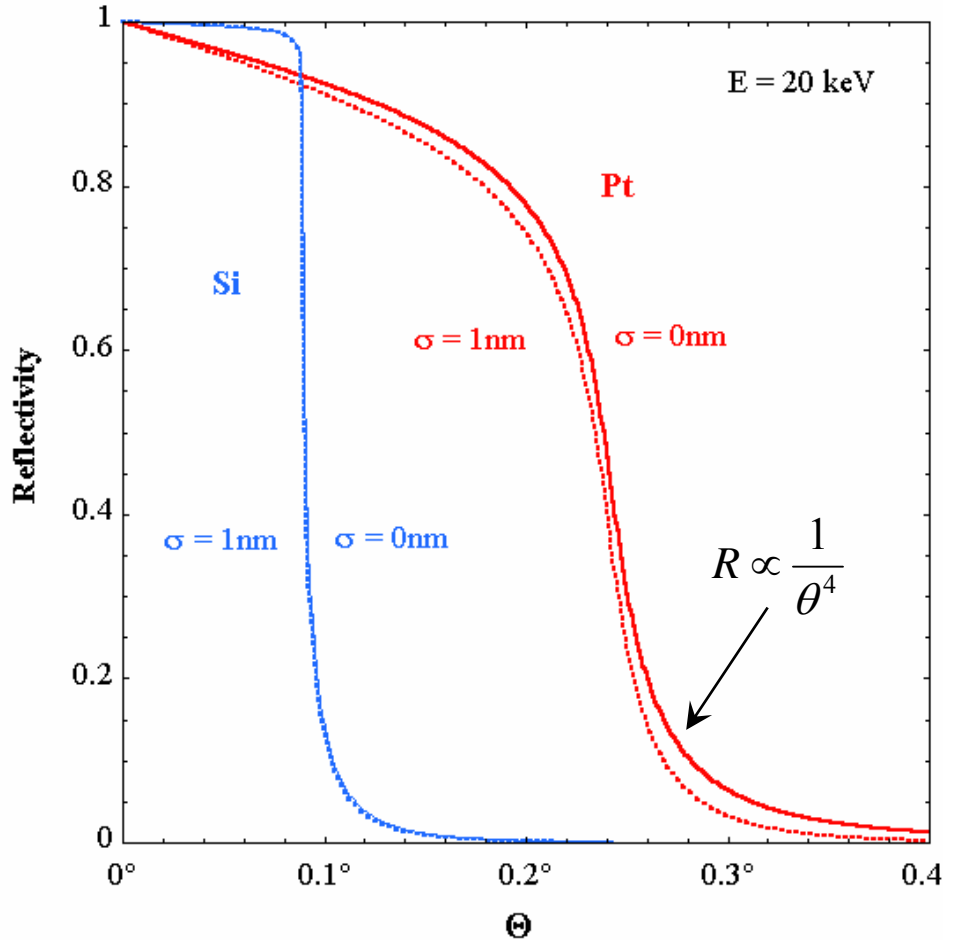
X-ray mirror reflectivity

Specular x-ray reflectivity at a surface

$$\theta_c = \sqrt{2 \cdot \delta} \propto \sqrt{\rho_e} \quad (\text{critical angle})$$

Important parameters

- Optical index $n = 1 - \delta + i\beta$
- Mass density ρ
- Interface width σ



X-ray multilayer reflectivity

Recursive calculation of Fresnel coefficients and propagation

- Parratt formalism (widely used in x-ray optics) [8]

Principle

- Start at semi-infinite substrate surface (no reflection from back side)
- Recursive construction of amplitudes and phases from layer to layer

$$r_{n-1,n} = a_{n-1}^4 \cdot \left[\frac{r_{n,n+1} + f_{n-1,n}}{r_{n,n+1} f_{n-1,n} + 1} \right]$$

$f_{n-1,n}$: Fresnel coefficients

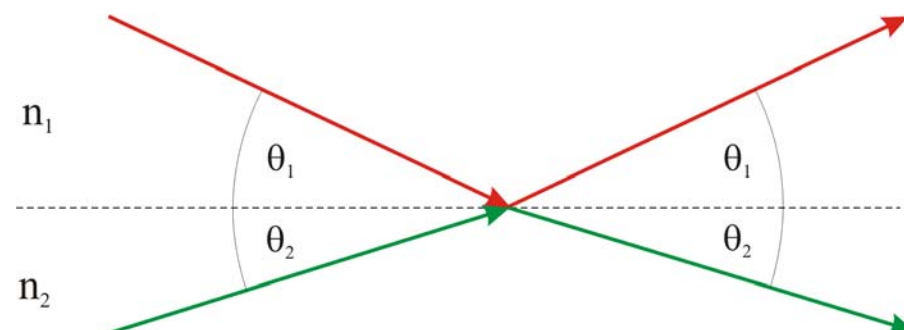
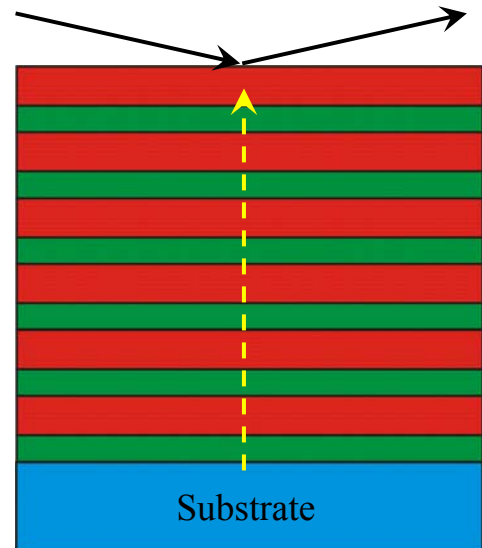
E_n : Electric field at centre of layer n

t_n : Thickness of layer n

$$r_{n,n+1} = a_n^2 \frac{E_n^R}{E_n}$$

$$a_n = e^{-i\frac{\pi}{\lambda}t_n\sqrt{n_n^2 - n_0^2 \cos^2 \theta}}$$

$$\rightarrow R = |r_{0,1}|^2$$



X-ray multilayer reflectivity

Numerical calculations

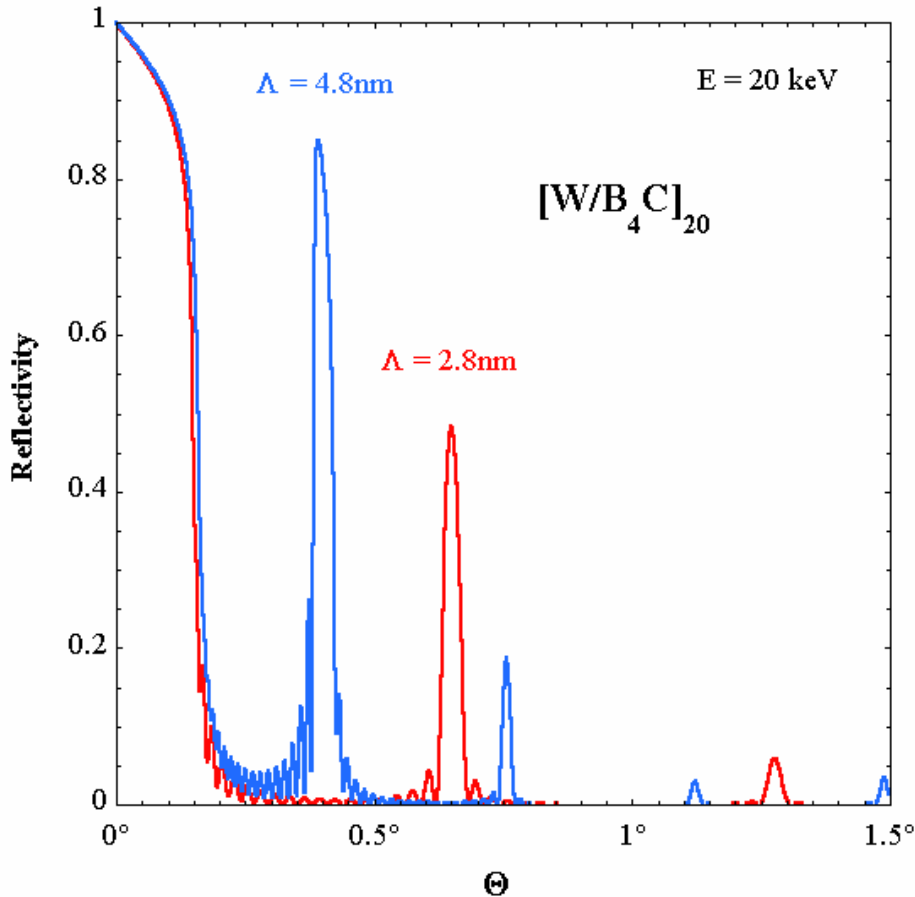
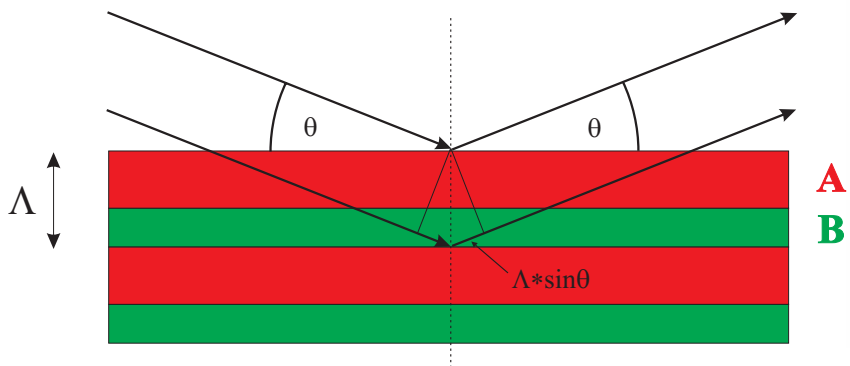
Main features

- Bragg peaks and fringes due to interference
- Positions depend on E and Λ
- Intensities depend on $\Delta\rho$, N, σ ...

Corrected Bragg equation

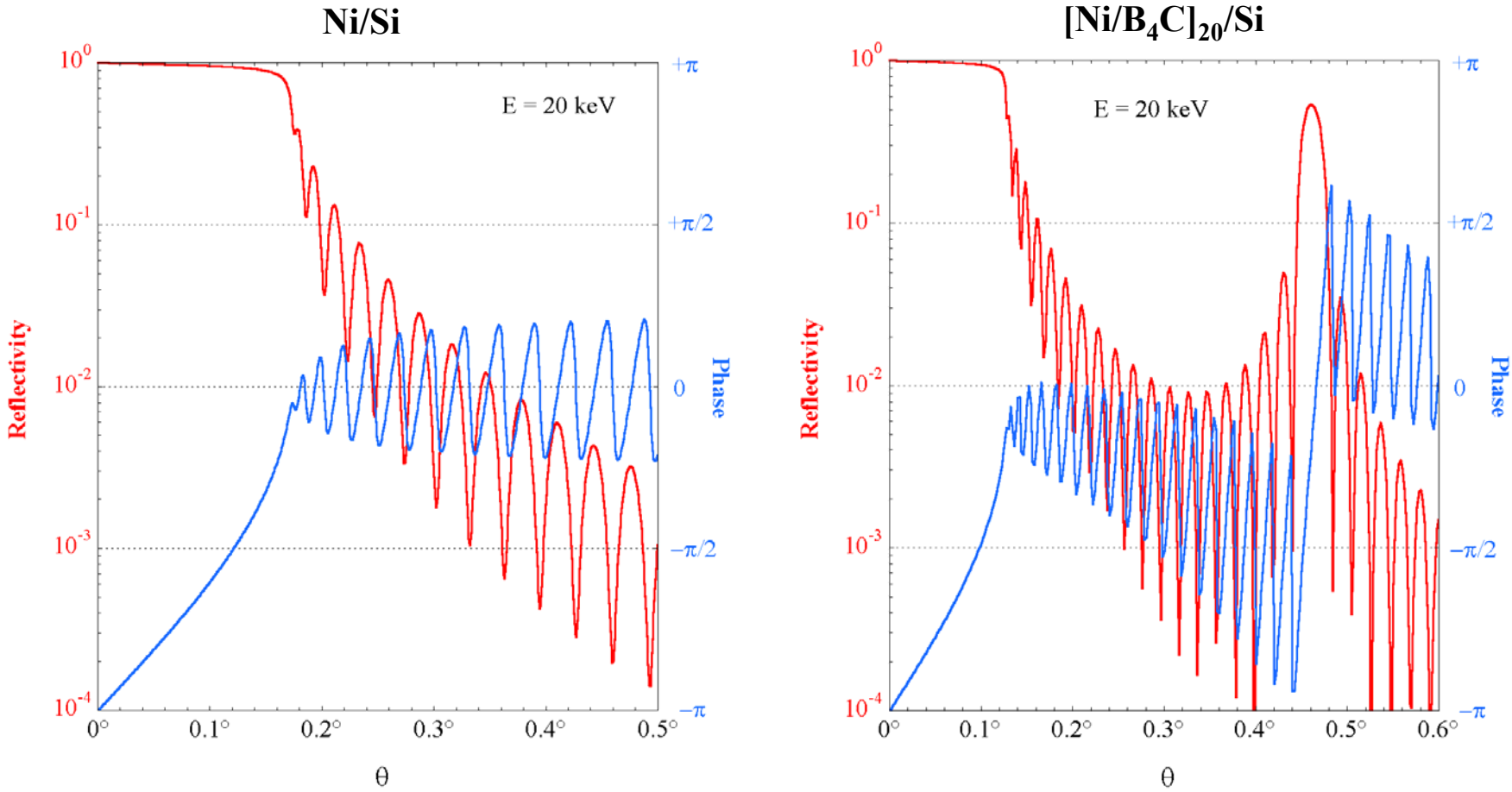
$$m \cdot \lambda = 2 \cdot \Lambda \cdot \sqrt{n_2^2 - n_1^2 \cos^2 \theta}$$

For $\theta \gg \theta_C \rightarrow m \cdot \lambda \approx 2 \cdot \Lambda \cdot \sin \theta$



X-ray reflectivity

Reflectivity and phase



X-ray multilayer reflectivity - Imperfections

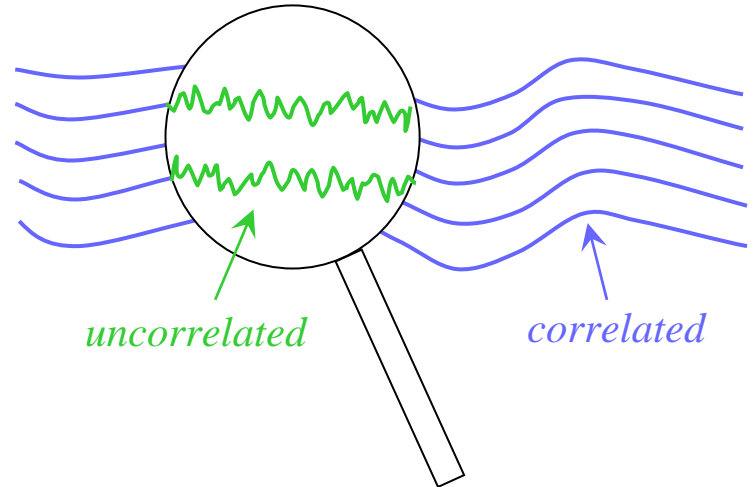
Interface roughness – Diffuse scattering

Kinematical (Born) Approximation (BA)

$$\frac{d\sigma}{d\Omega} = \left(\frac{r_e \rho}{q_z} \right)^2 \left(\frac{A}{\sin \theta_{in}} \right) \cdot \int e^{-q_z \cdot g(x,y)/2} \cdot e^{i(q_x x + q_y y)} dx dy$$

Height differences $g(x, y) = \langle (h(0,0) - h(x, y))^2 \rangle$

Uncorrelated interfaces $\frac{d\sigma}{d\Omega} = \frac{d\sigma}{d\Omega} \Big|_{Fresnel} \cdot e^{-q_z^2 \sigma^2}$



- Scattering remains specular
- Reflectivity cannot distinguish density gradient from uncorrelated roughness

Correlated interfaces

- Generally numerical solutions, few analytical cases
- Non-specular scattering
- Information on lateral interface structure

X-ray multilayer reflectivity - Imperfections

Interface roughness – Diffuse scattering

Distorted Wave Born Approximation (DWBA)

$$\frac{d\sigma}{d\Omega} = \frac{A}{\sin \theta_i} \frac{\pi^2}{\lambda^4} (1-n^2)^2 \cdot |t_i|^2 \cdot |t_f|^2 \cdot PSD(\vec{q})$$

Power spectrum density $PSD(\vec{q}) = \int C(\vec{r}) \cdot e^{i\vec{q}\vec{r}} d\vec{r}$

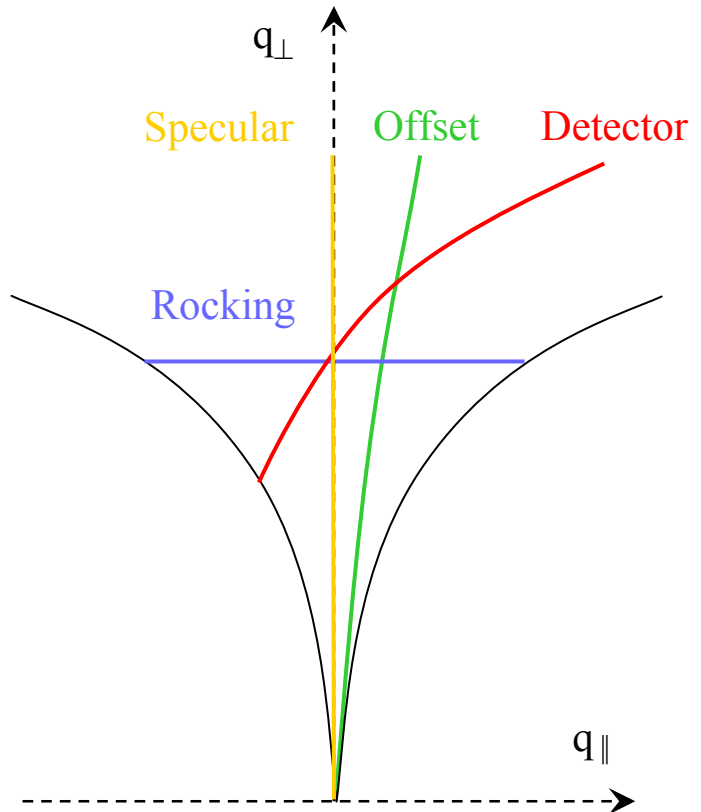
Height correlation function $C(\vec{r}) = \langle h(\vec{r}) \cdot h(\vec{r}') \rangle$

- Refraction included → “Yoneda wings”
- Various approaches for PSD
- Complicated computation for multilayers

Theory and software

- S.K. Sinha, V. Holy, D.K.G. de Boer, T. Salditt
- IMD (D. Windt)

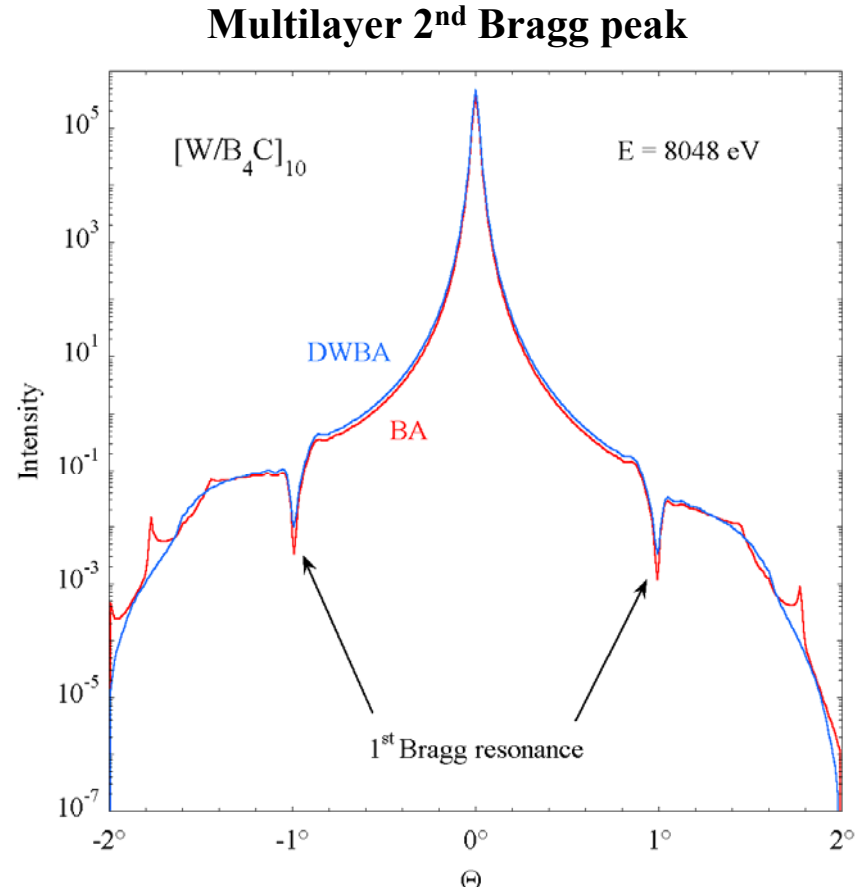
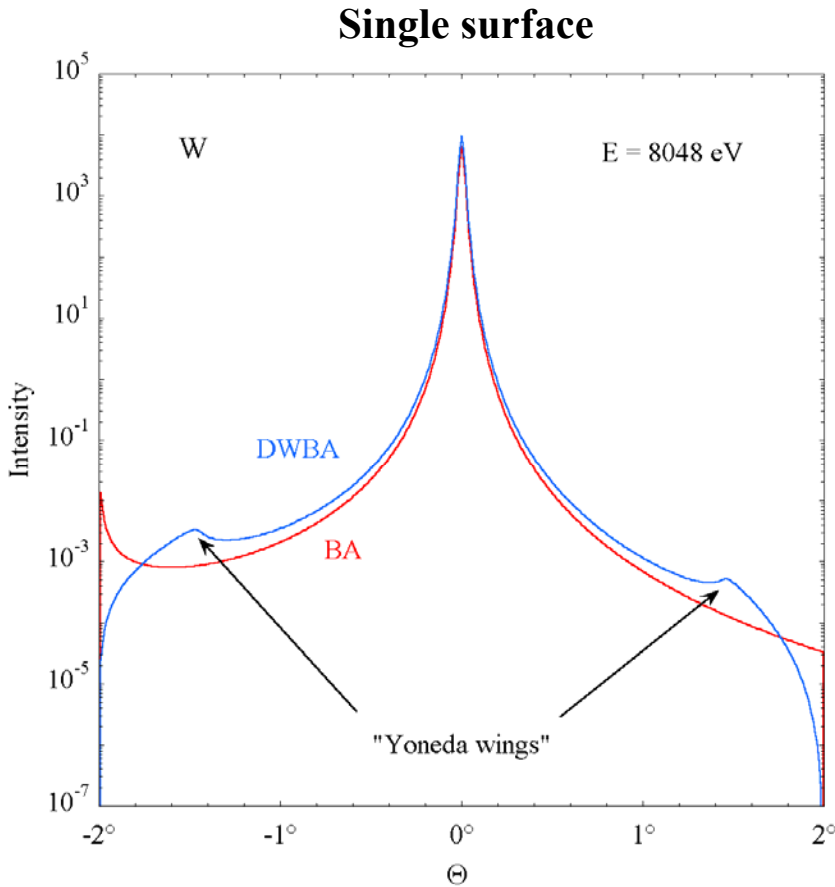
Scattering geometries



X-ray multilayer reflectivity - Imperfections

Diffuse scattering – Comparison: BA – DWBA

IMD (D. Windt)



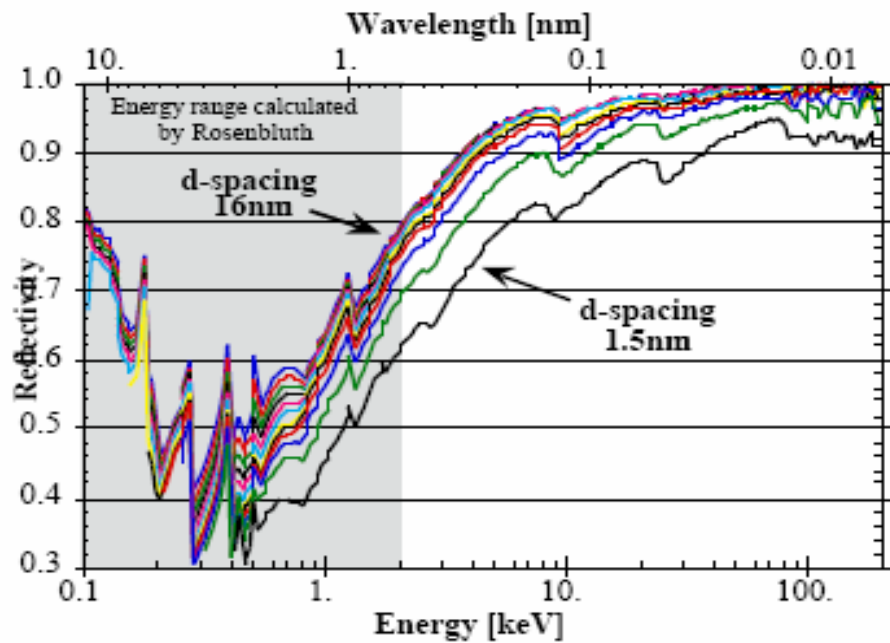
X-ray multilayer design

Materials choice – Basic rules:

1. Select low-Z spacer material with lowest absorption (β_{spacer})
2. Select high-Z absorber material with highest reflectivity with spacer ($\delta_{\text{abs}} - \delta_{\text{spacer}}$)
3. In case of multiple choices select high-Z material with lowest absorption (β_{abs})
4. Make sure that both materials can form stable and sharp interfaces (lower d-spacing limit)

Computational search algorithms

- Soft X-rays: A.E. Rosenbluth (1988)
- Hard X-rays: K. Vestli (1995)



[9] K. Vestli, E. Ziegler, Rev. Sci. Instr. 67, 3356 (1996)

X-ray multilayer design

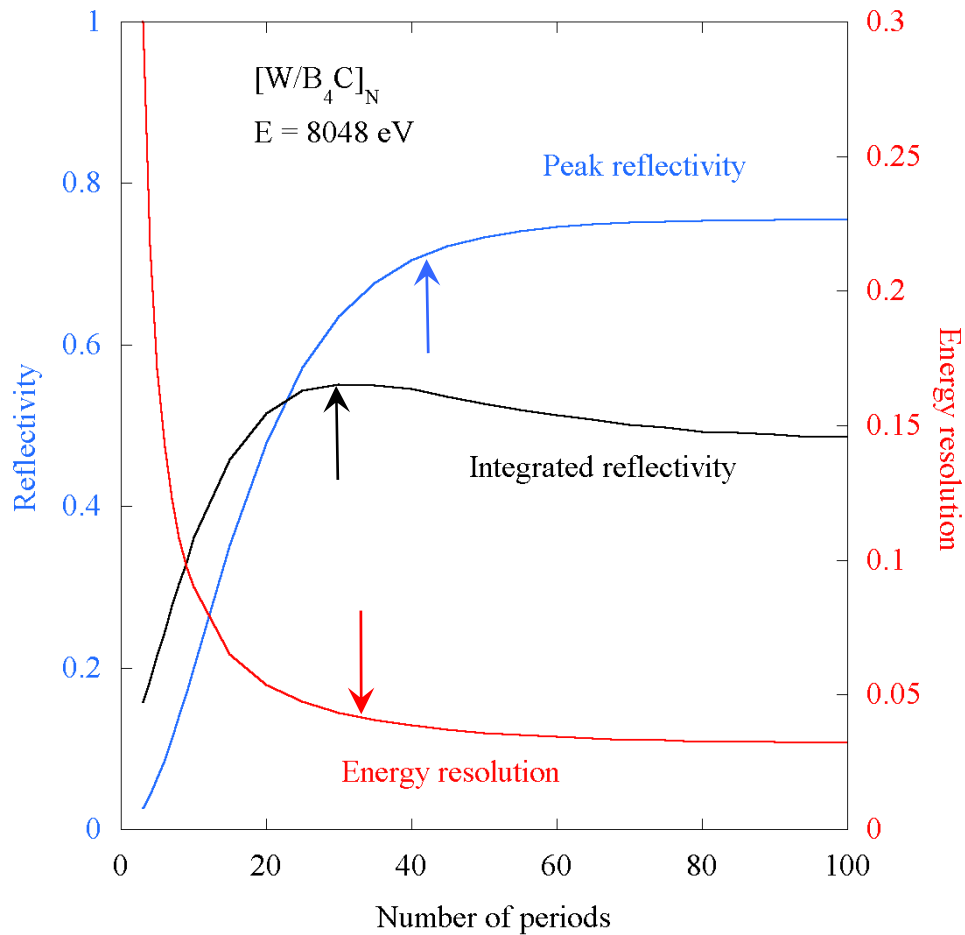
Period number N:

Peak versus integrated reflectivity:

- R_{peak} increases with N up to extinction
- $\Delta E/E$ decreases $\sim 1/N$ in kinematical range
- R_{int} is maximum before extinction

High and low resolution MLs

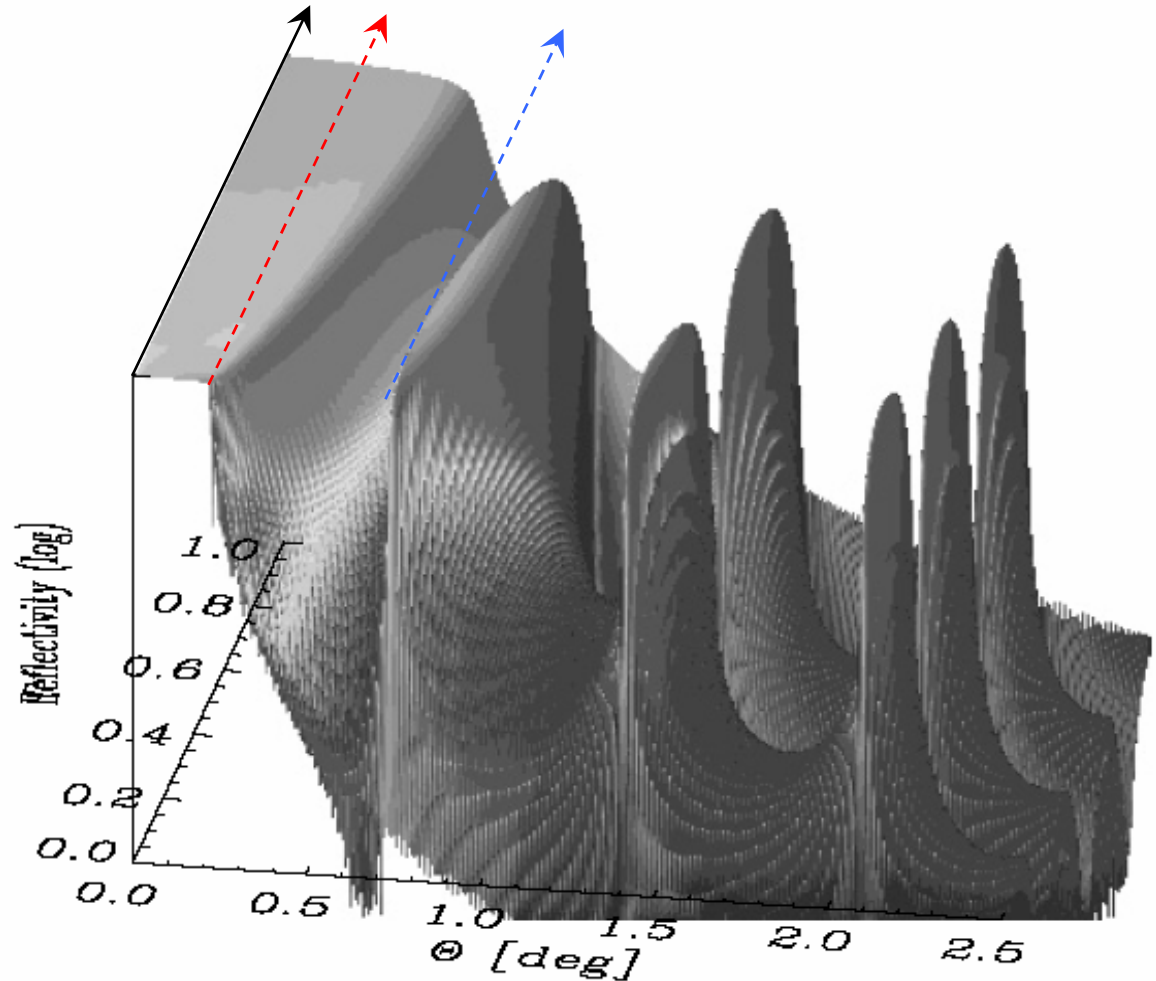
Optimize N according to needs !



X-ray multilayer design

Filling factor $\Gamma = t_{\text{abs}}/\Lambda$

- Harmonics suppression
- Reflectivity enhancement

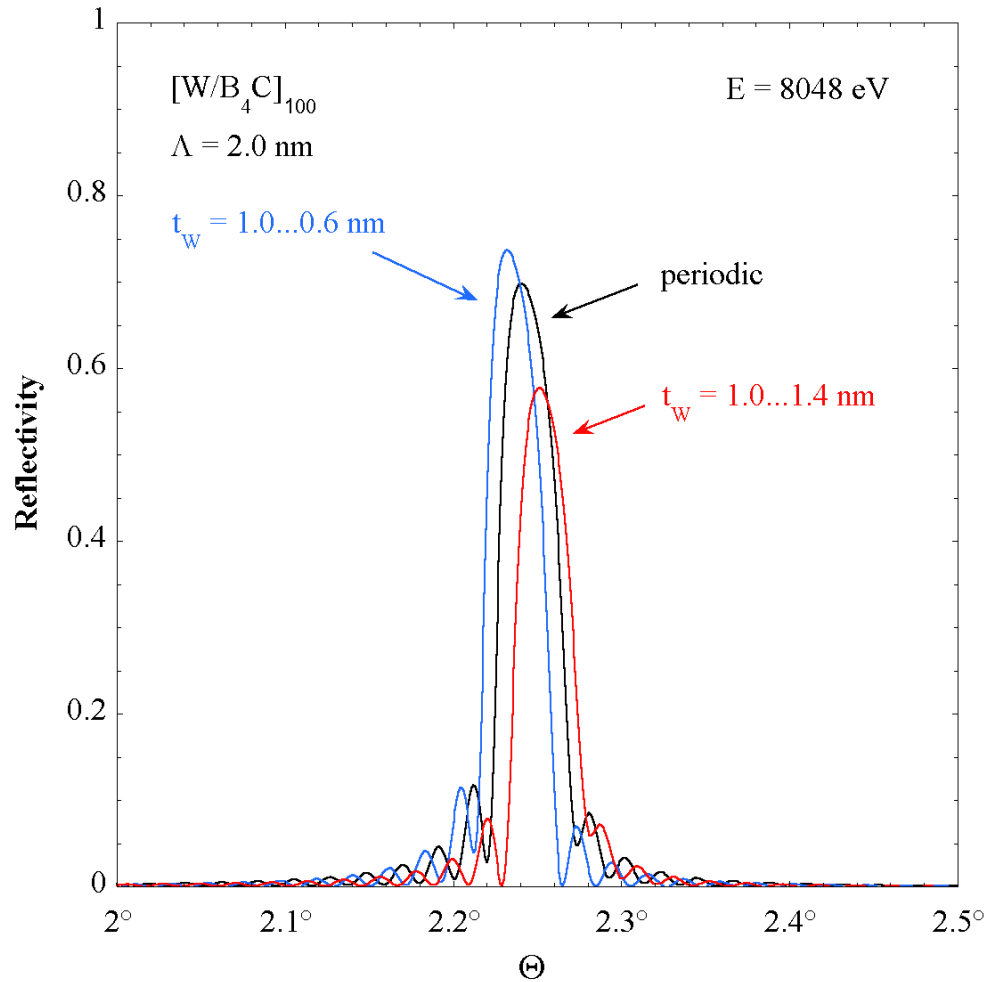
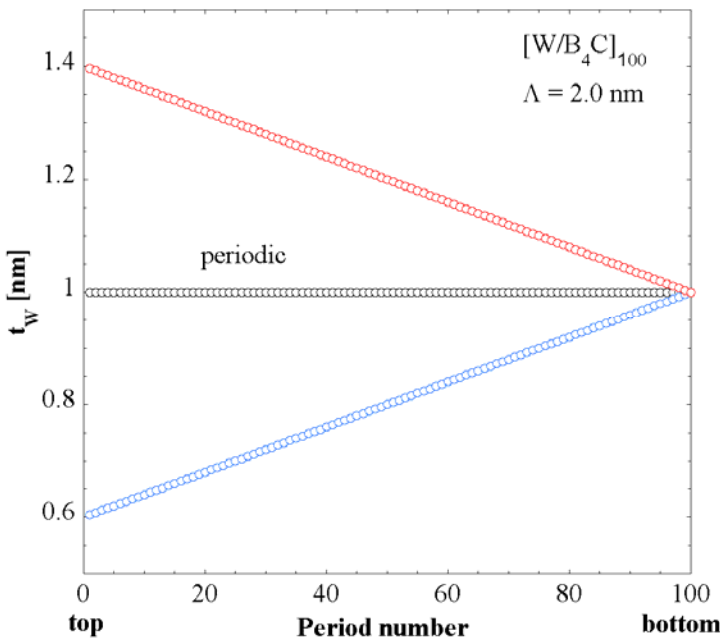


X-ray multilayer design

Quasi-periodic design:

Simple approach

- Constant d-spacing
- Decreasing Γ from 0.5 at bottom to top



X-ray multilayer design

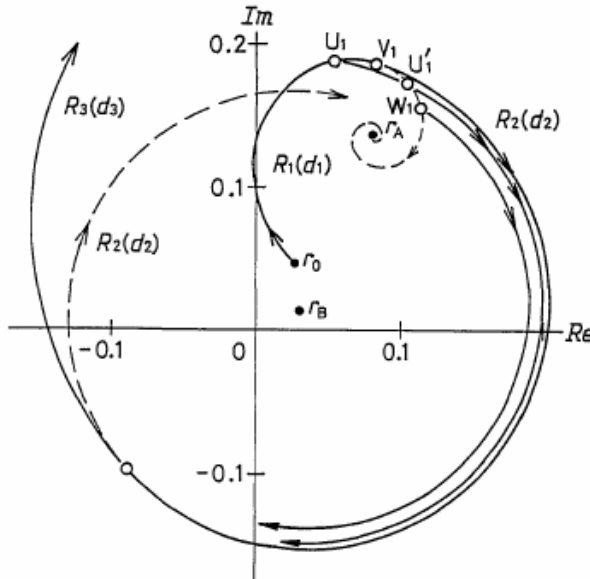
Aperiodic design:

Layer-by-layer design (M. Yamamoto)

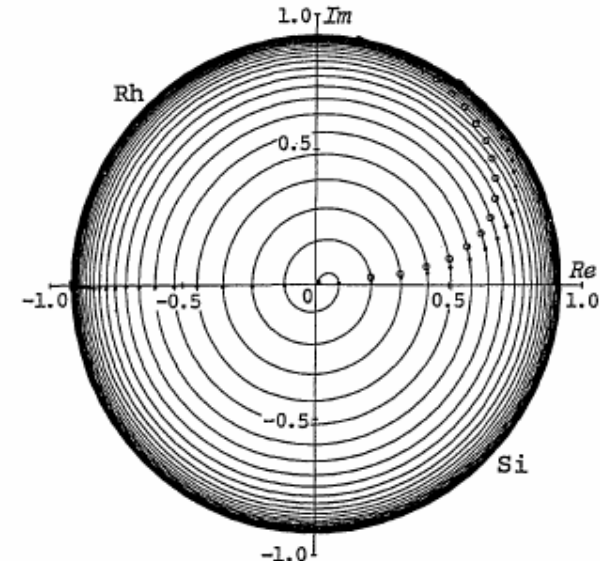
- Amplitude maximization with respect to vacuum
- Berning's recursive formula
- Non-periodic structure

$$r_n = \frac{f_n(1 - f_n r_{n-1}) + (r_{n-1} - f_n)e^{-i\varphi_n}}{1 - f_n r_{n-1} + f_n(r_{n-1} - f_n)e^{-i\varphi_n}}$$

$$\varphi_n = e^{-i4\pi \frac{t_n}{\lambda} \sqrt{n_n^2 - n_0^2 \cos^2 \theta}}$$



[11] M. Yamamoto, T. Namioka, Appl. Opt. 31, 1622 (1992)



X-ray multilayer design

Aperiodic design:

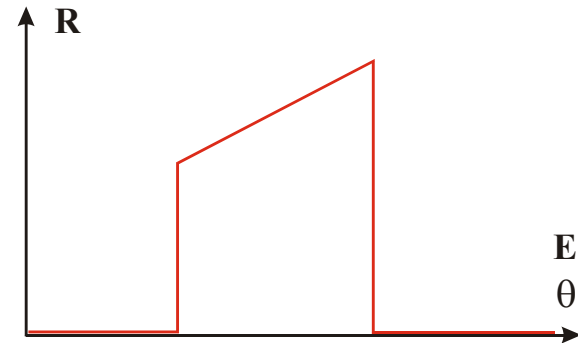
Goal: ML with particular reflectivity profile

- $R = R(\theta)$ for $E = \text{const}$
- $R = R(E)$ for $\theta = \text{const}$

Find vertical composition profile

Method:

- Derive analytical expression for reflectivity
- Do inversion to obtain 1st estimate for layer sequence
- Apply fit algorithm to optimize the structure



[12] I.V. Kozhevnikov et al, Nucl. Instr. And Meth. A 460, 424 (2001)

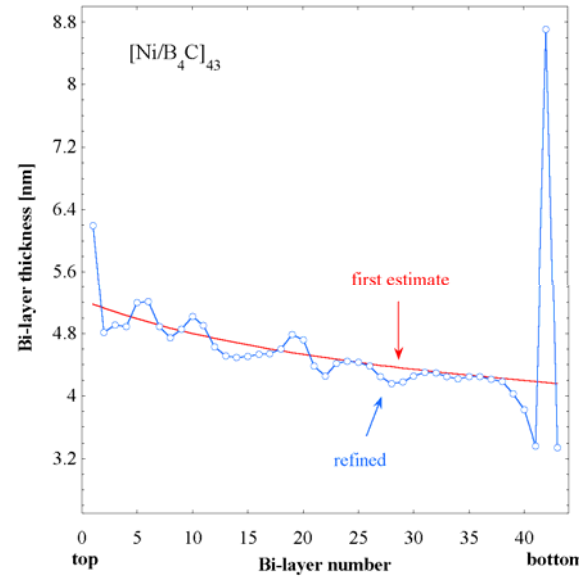
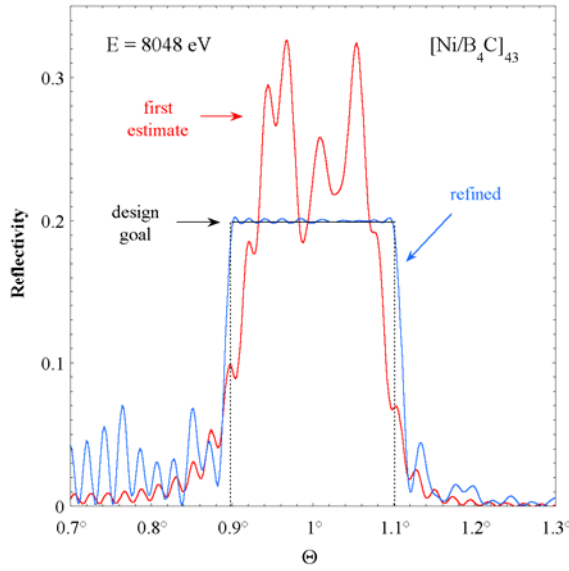
X-ray multilayer design

Example:

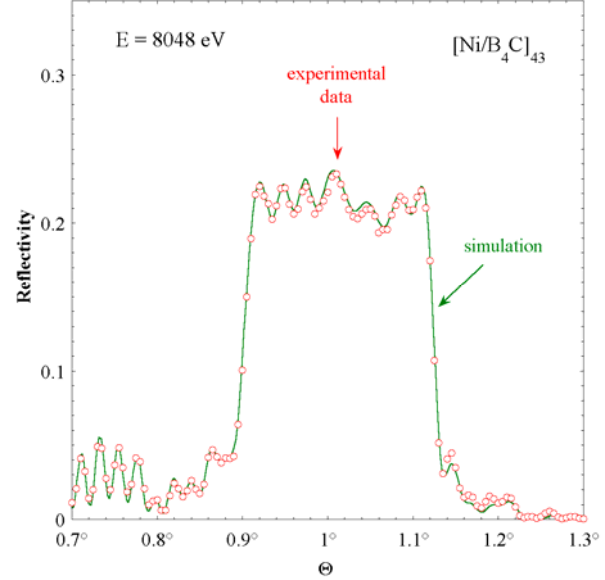
- Ni/B₄C structure
- R(θ) = const over 20% bandwidth

[13] Ch. Morawe et al, Nucl. Instr. And Meth. A 493, 189 (2002)

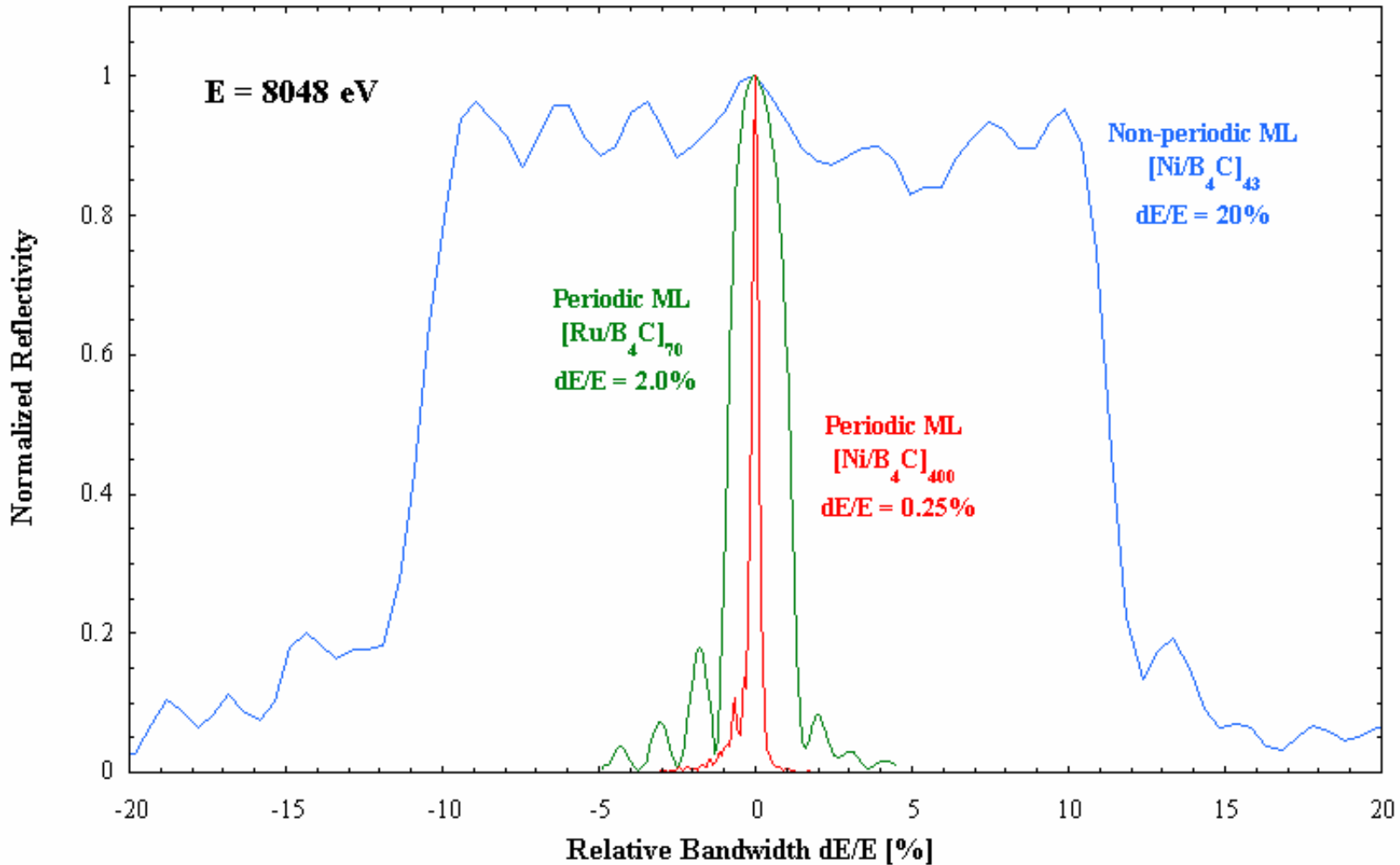
Theoretical design



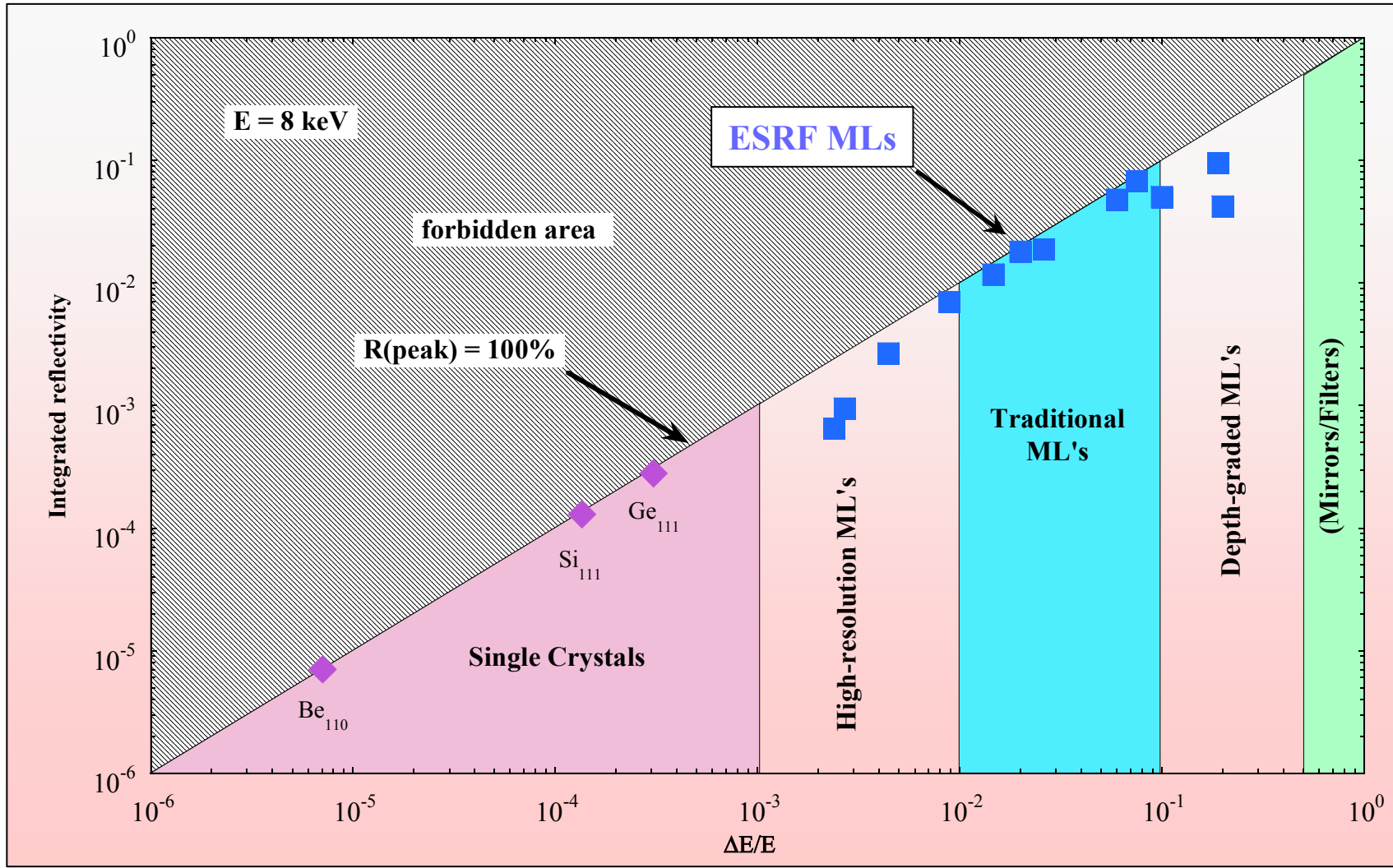
Experimental result



Energy resolution of multilayers

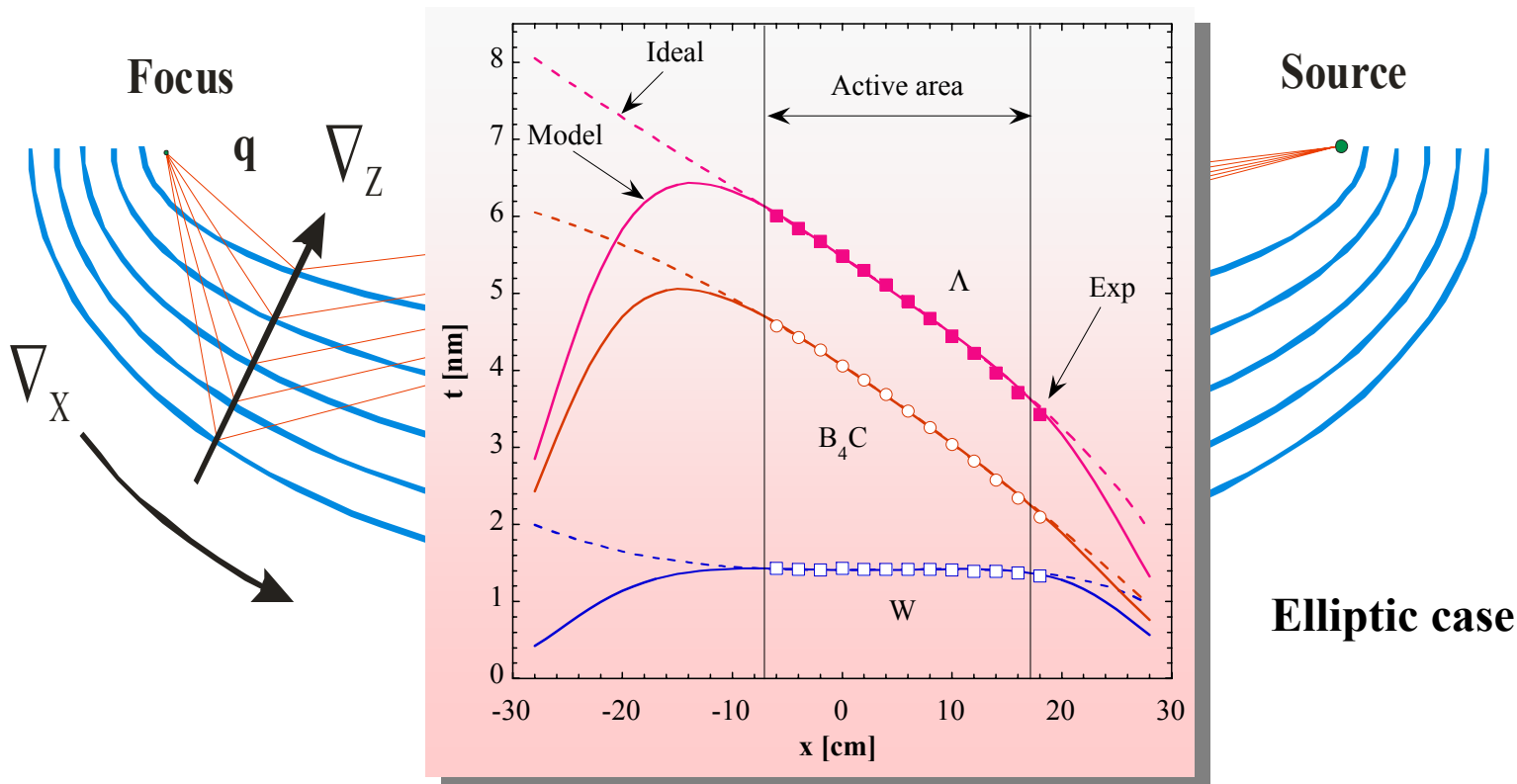


Reflecting X-ray optics – Overview



Laterally graded multilayers

- Divergent beam, focusing applications with curved substrates
- Incidence angle variation → laterally graded multilayers
- Additional depth gradient negligible ($< 10^{-5}$)



Laterally graded multilayers

Surface curvature and beam divergence define lateral gradient $d\Lambda / dx$

Shape

Parabolic

Elliptic

Flat

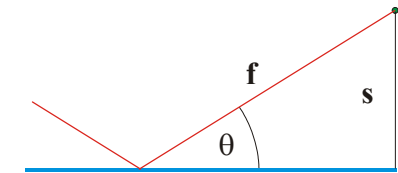
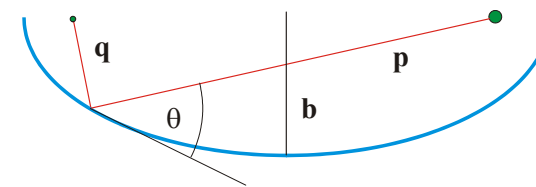
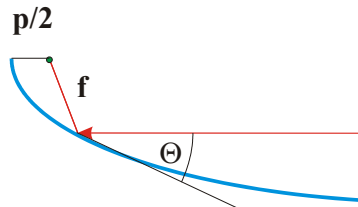
Angle θ

$$\sin \theta = \sqrt{\frac{p}{2f}}$$

$$\sin \theta = \frac{b}{\sqrt{pq}}$$

$$\sin \theta = \frac{s}{f}$$

Geometry



**d-spacing including refraction correction
(modified Bragg equation)**

$$\Lambda = \frac{\lambda \cdot m}{2\sqrt{n^2 - \cos^2 \theta}}$$

Double graded multilayers

Energy dispersion:

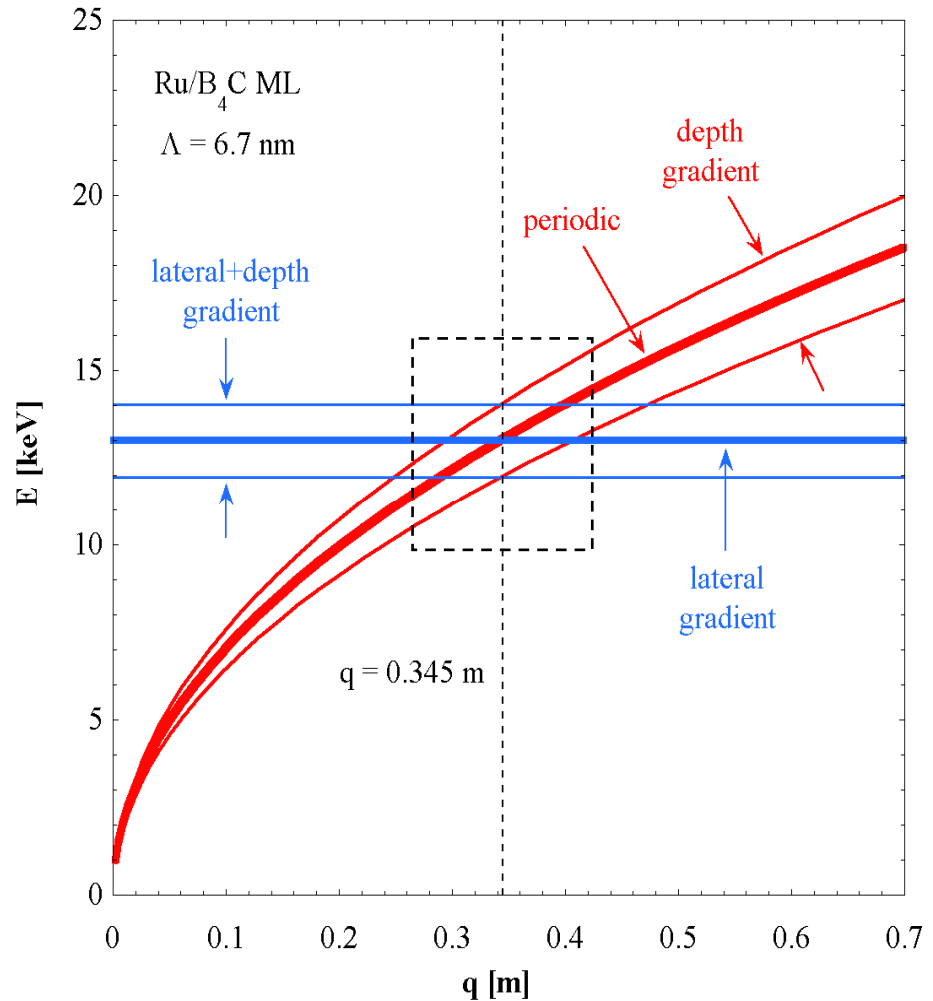
Bragg equation: $E(\theta) = \frac{h \cdot c}{2\Lambda \sqrt{n^2(E) - \cos^2 \theta}}$

Elliptic mirror: $\sin^2 \theta = \frac{b^2}{p \cdot q} \quad p + q = 2 \cdot a$



$$E(q) = \frac{h \cdot c}{2\Lambda \sqrt{n^2(E) - 1 + \frac{b^2}{(2a-q)q}}}$$

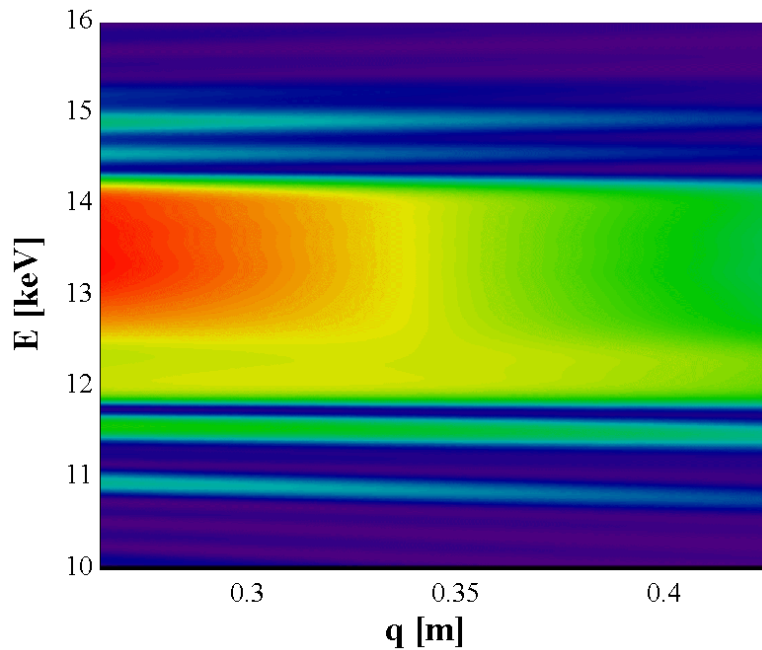
Dispersion “along ML mirror”



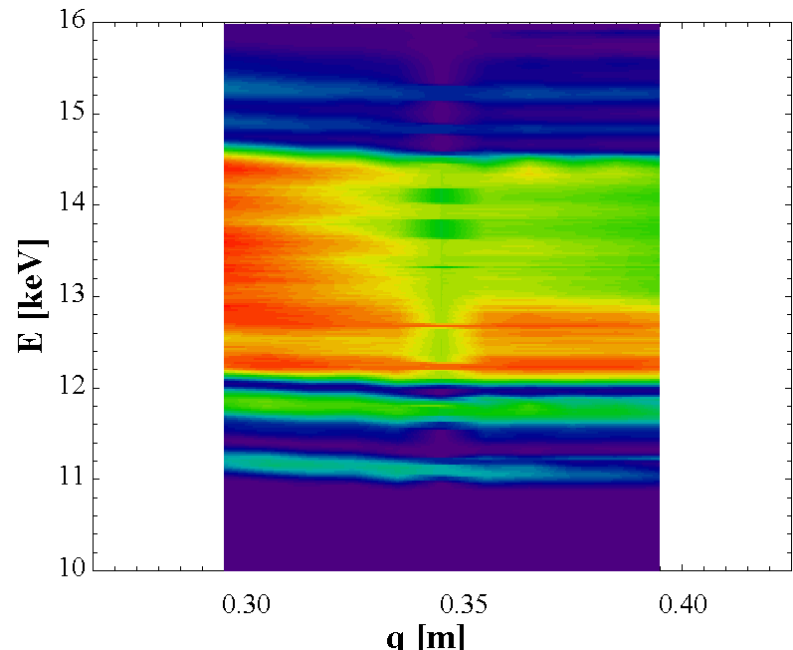
Double graded multilayers

Intensity profiles: (Kirkpatrick-Baez multilayer optics on ESRF BM05)

Theory



Experiment



[14] Ch. Morawe, Ch. Borel, E. Ziegler, J-Ch. Peffen, Proc SPIE 5537, 115 (2004)

X-ray multilayer fabrication

Deposition techniques	Vacuum	Particle energy	Deposition rate	Deposition area
Thermal evaporation	HV (UHV)	Low	Low	Small
E-beam evaporation	UHV	Low	Low	Small
Magnetron sputtering	HV (+Gas)	High	High	Large
DECR sputtering	HV (+Gas)	High	Low	Medium
Ion beam sputtering	UHV (+Gas)	Very high	High	Medium
Pulsed laser deposition	HV	Very high	High	Medium

- Characteristics may vary depending on equipment and application
- Magnetron sputtering most widely used for X-ray multilayer fabrication
- Vacuum and purity important for EUV and soft X-rays
- High particle energy favors very thin and uniform layers

X-ray multilayer fabrication

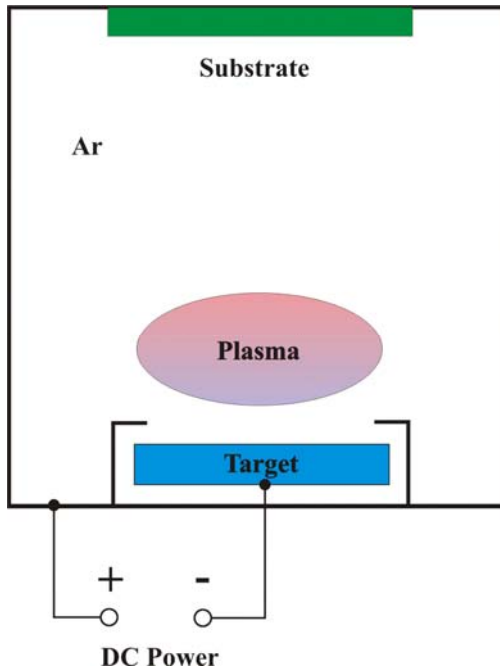
History

1923	Koeppe	Cd/Ag	electrolysis	unstable
1930	Deubner	Au/Ag	electrolysis	unstable
1935	Dumond	Au/Cu	thermal evaporation	1 week life time
1963	Dinklage	Me/Mg	thermal evaporation	stable
1972	Spiller	Au/MgF ₂	thermal evaporation	UV MLs
1976	Haelbich	Me/C	thermal evaporation	XUV MLs
1978	Barbee	W/C	magnetron sputtering	X-ray MLs
1983	Gaponov	Me/C	pulsed laser deposition	X-ray/VUV MLs

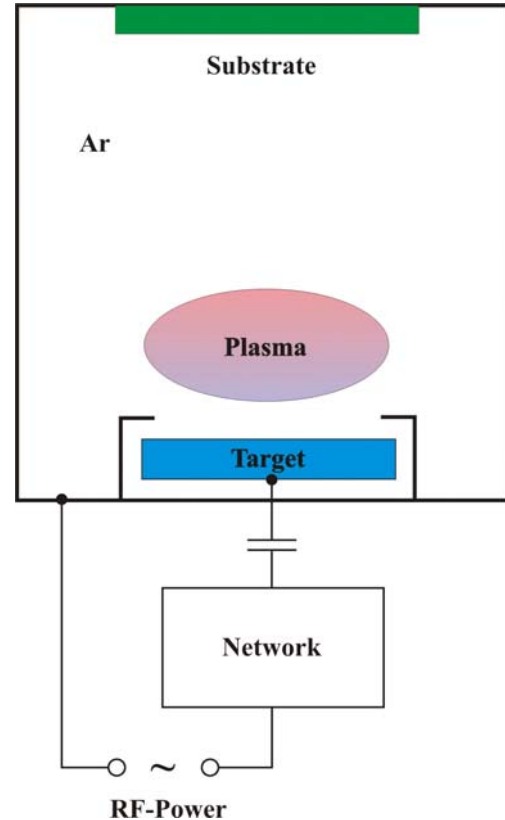
X-ray multilayer fabrication

Sputtering techniques

DC (conductors)



RF (insulators)

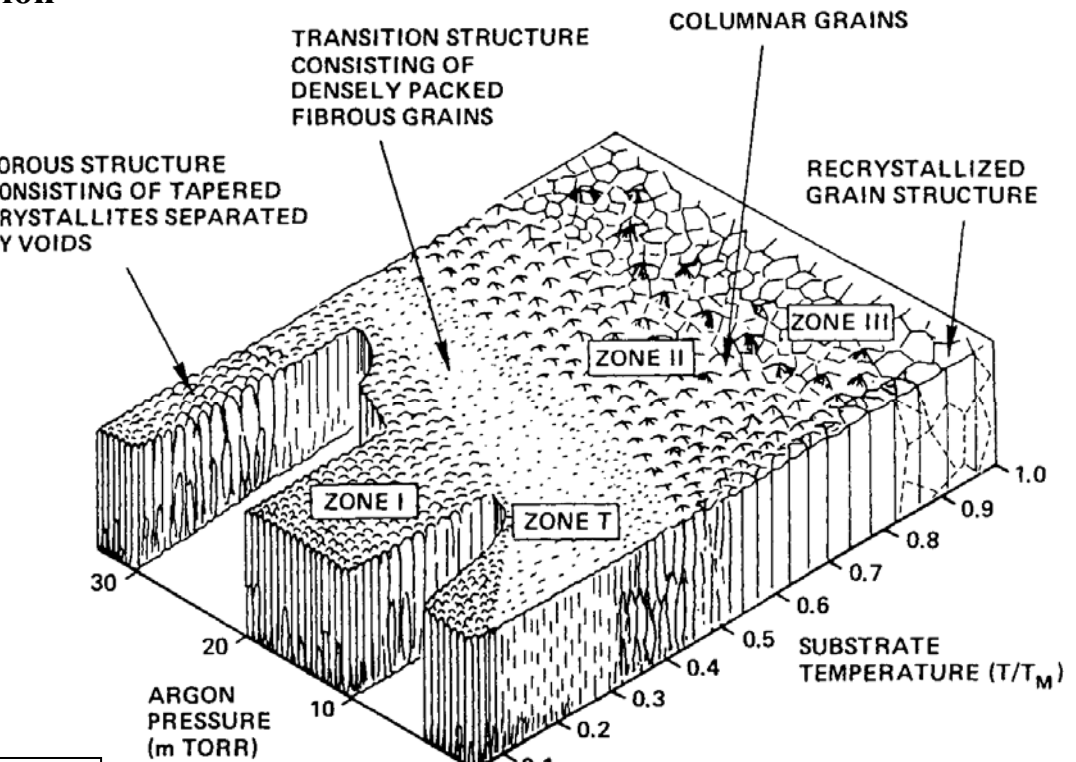


X-ray multilayer fabrication

Thin film growth

- Good adhesion
- Trade-off: in- and out-of-plane diffusion
- Preference for amorphous layers
- Low working gas pressure
- Low substrate temperature
- Consider interface chemistry

Thornton zone model for sputtering

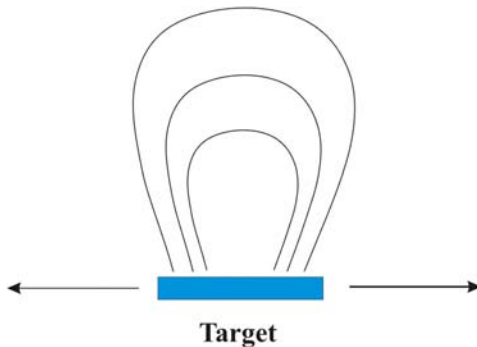
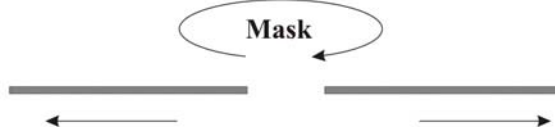
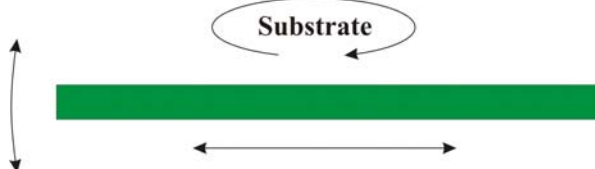


[15] J.A. Thornton, Ann. Rev. Mater. Sci. 7, 239 (1977)

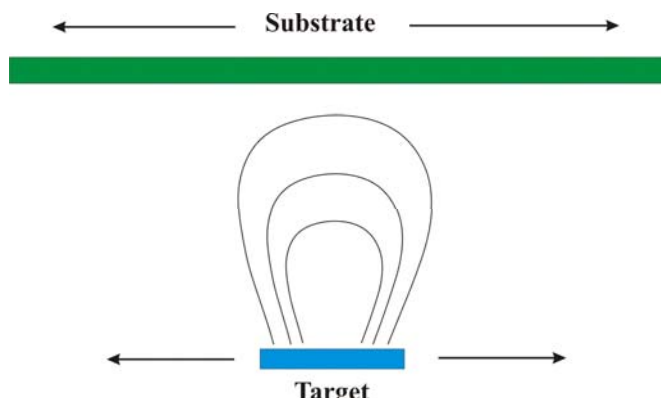
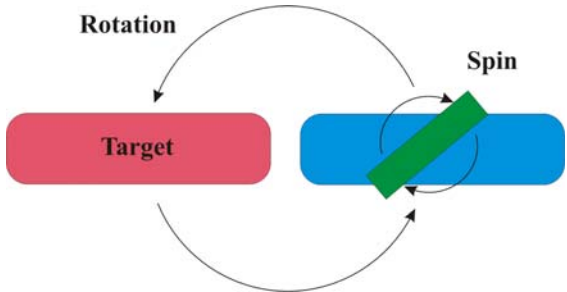
X-ray multilayer fabrication

Large area coatings (uniform, gradient)

- Relative motion source - substrate
- Masking techniques

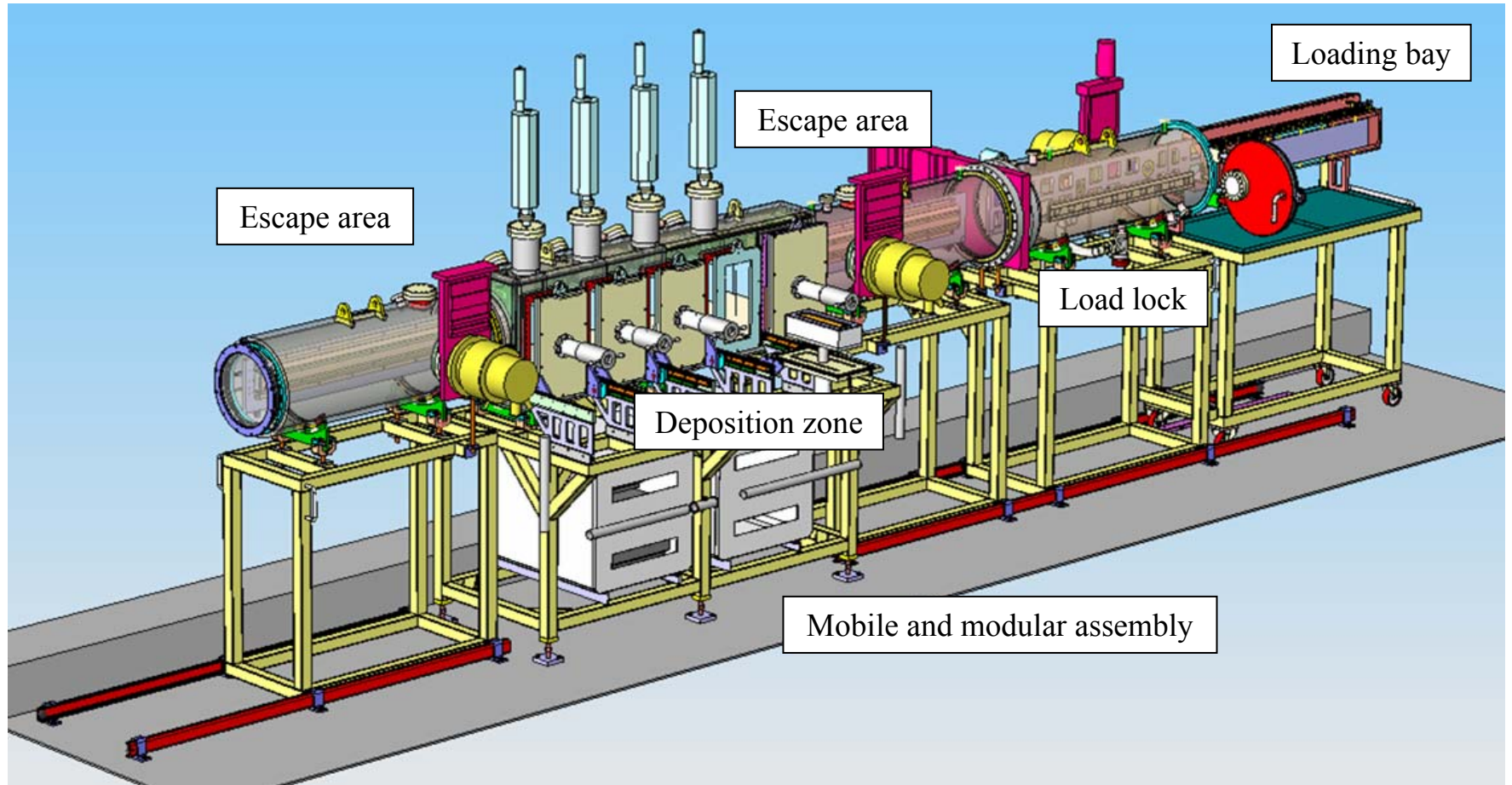


$$t(\vec{r}) = \int \varphi(\vec{r}, \vec{r}') \frac{d\vec{r}'}{v(\vec{r}')}$$



X-ray multilayer fabrication

ESRF magnetron sputter deposition system



X-ray multilayer fabrication

Technology and engineering

Curved MLs

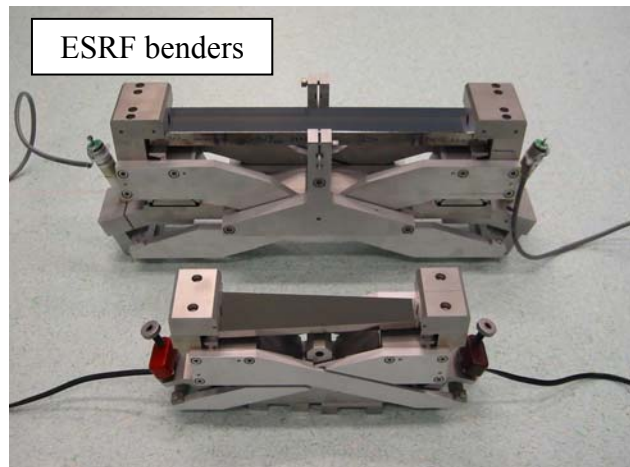
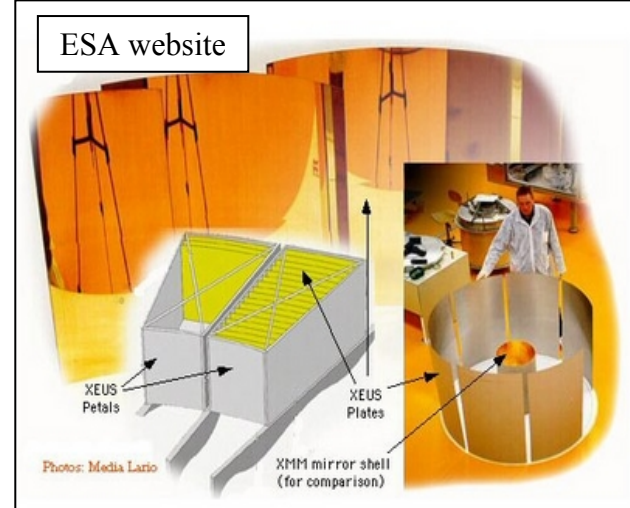
- Figured substrates or bending techniques ?
- Surface finishing (deterministic polishing/etching/coating)
- Weight and aperture (astronomy)

Stability and stress

- Intrinsic stress after coating (mainly compressive)
- Thermal and radiation load (white beam)
- Protection against debris (EUV, laser plasma, astronomy)
- Sample environment (vacuum/He/N₂)

Interface engineering

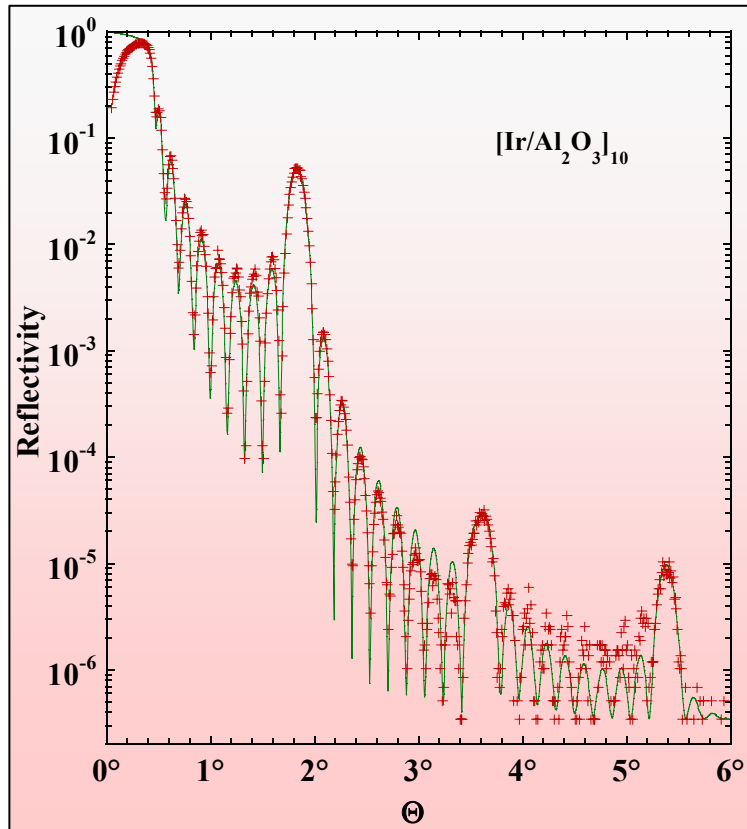
- Cap and barrier layers (EUV)



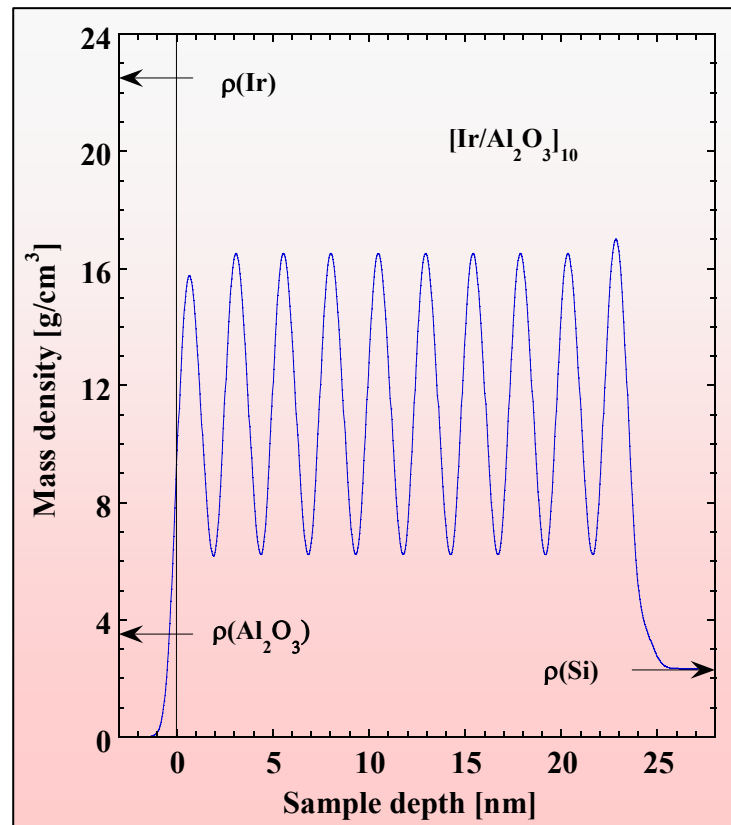
X-ray multilayer characterization

X-ray reflectivity

Simulation of x-ray reflectivity



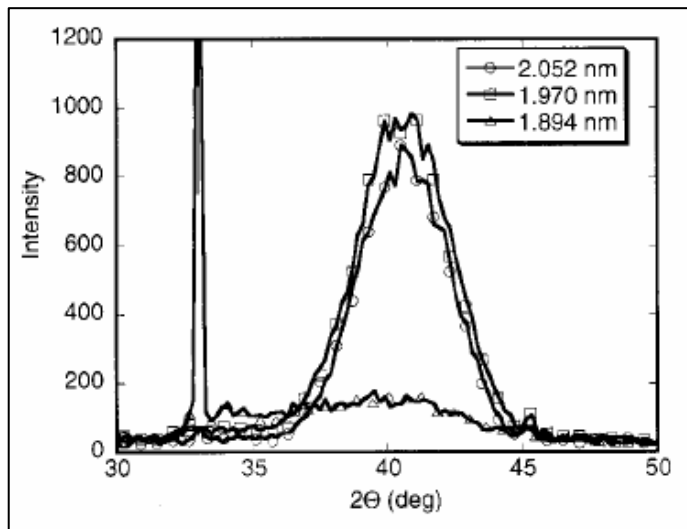
Vertical density profile



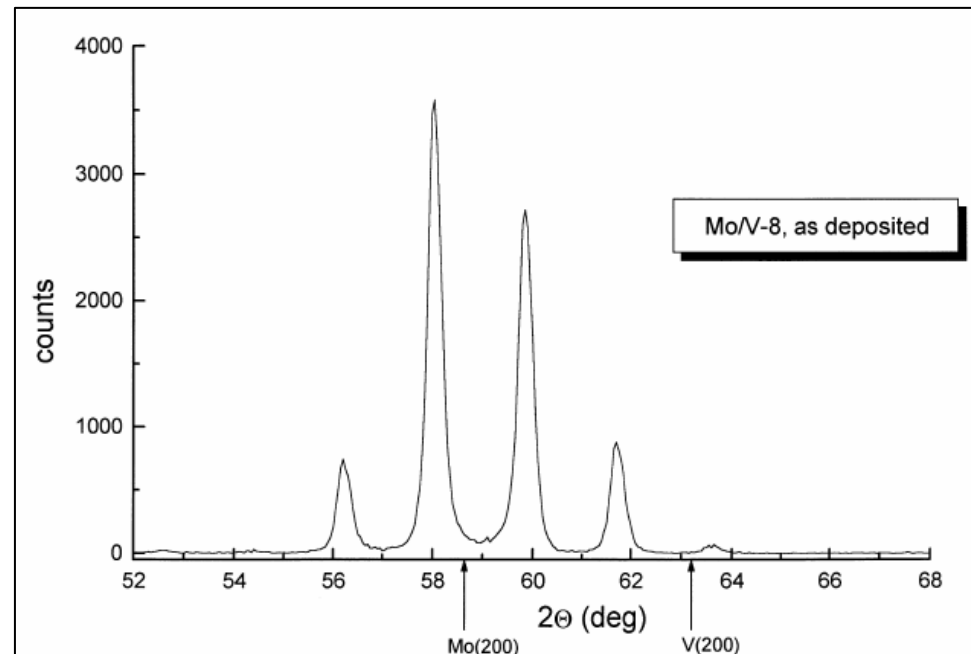
X-ray multilayer characterization

X-ray scattering

- Access to atomic structure
- Phase transitions
- Coherence lengths
- Superlattice formation



[16] S. Bajit et al, J. Appl. Phys. 90, 1017 (2001)



[17] D.L Beke et al, Vacuum 50, 373 (1998)

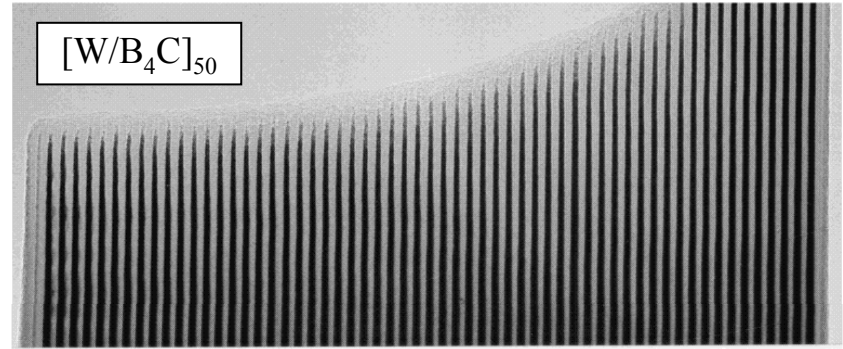
X-ray multilayer characterization

Transmission electron microscopy (TEM)

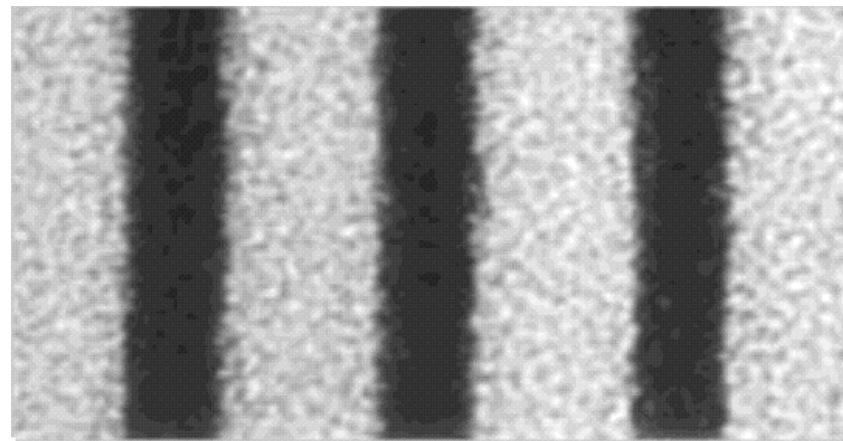
- Fabrication errors
- Roughness evolution
- Crystallinity
- Interface diffusion



Complementary to x-ray measurements !



100 nm



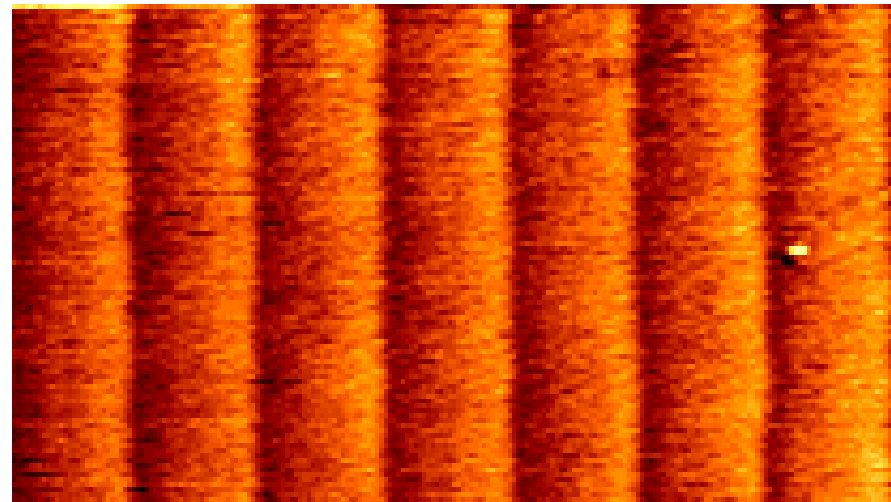
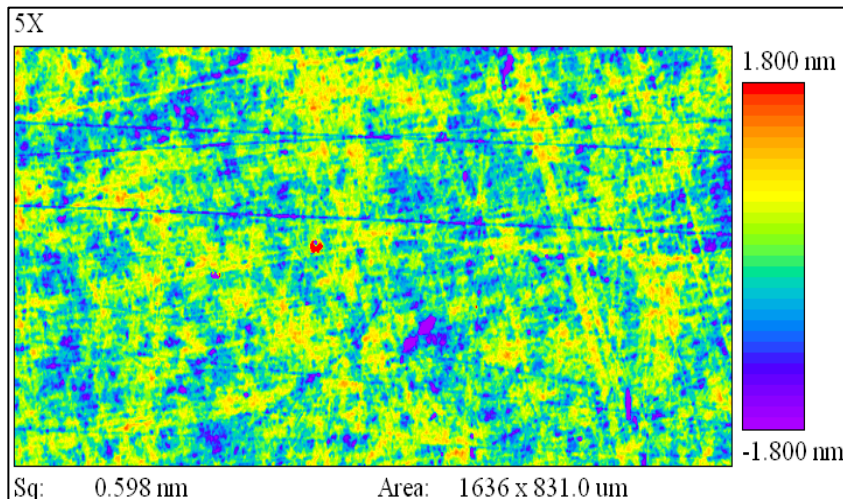
R. Scholz, MPI Halle, Germany

X-ray multilayer/mirror characterization

Surface metrology

- Atomic Force Microscopy (AFM)
- Interferometry
- Long Trace Profiler (LTP)
- From nm to m scale
- No depth information !

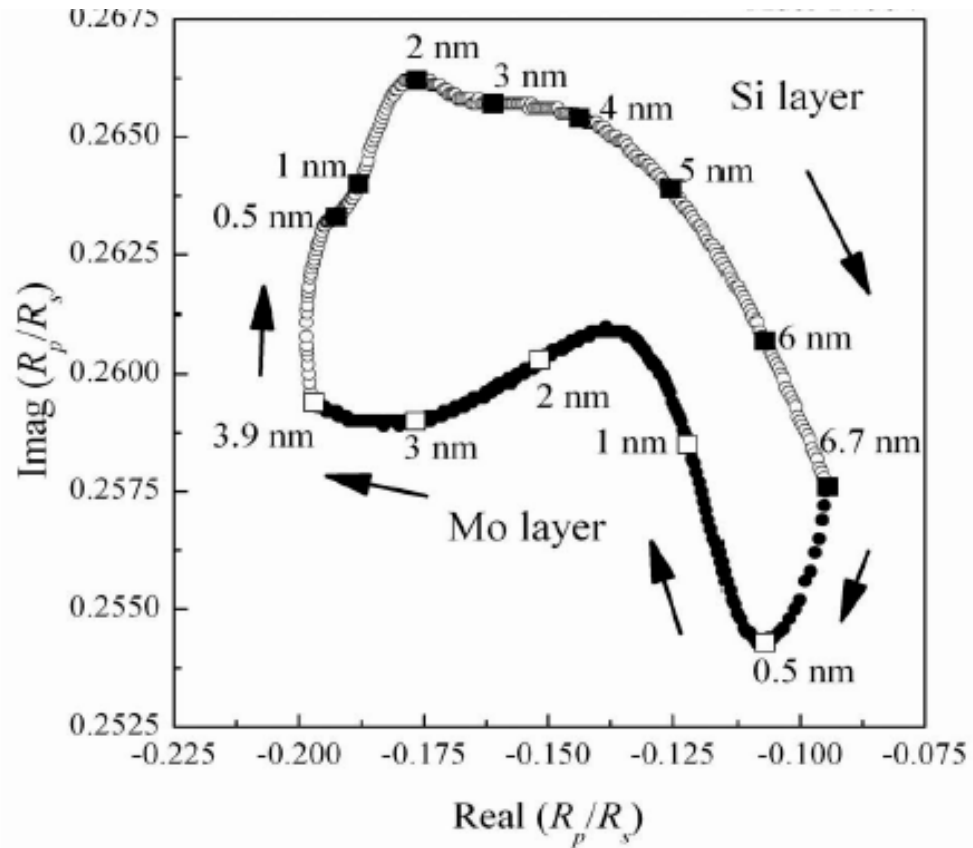
A. Rommevaux, ESRF Optics Group



X-ray multilayer characterization

Ellipsometry

- Complex field amplitude
- In-situ tool during growth
- Based on growth models
- Access to nucleation/coalescence
- Limited penetration depth !

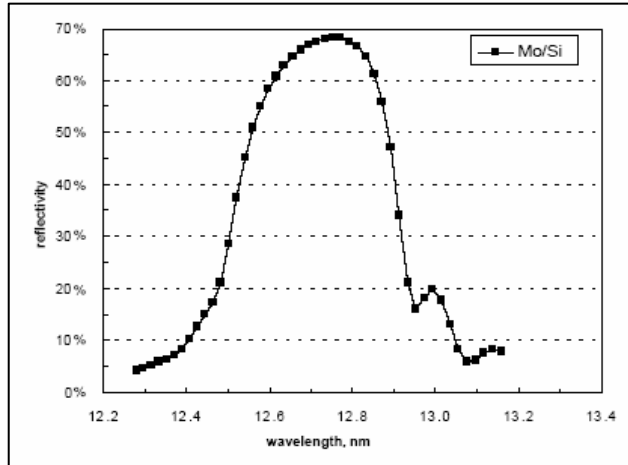


[18] T. Tsuru, T. Harada, M. Yamamoto, IPAP Conf. Series 7, 168 (2006)

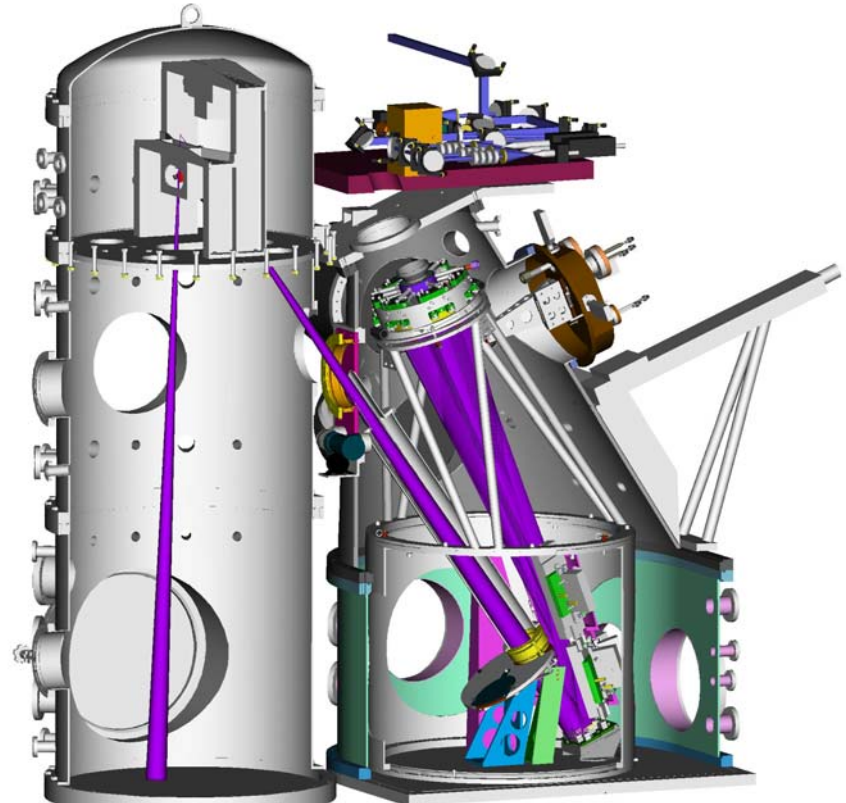
Applications

EUV lithography

- Vast projects in U.S. and Europe
- Achieve 30 nm structures on chips
- Illumination at $\lambda = 13.4$ nm
- Multilayer based optics
- Near normal incidence
- ≈ 10 reflections $\rightarrow R = R_i^{10} !$
- Mo/Si and derivatives most promising



Sandia National Laboratory website

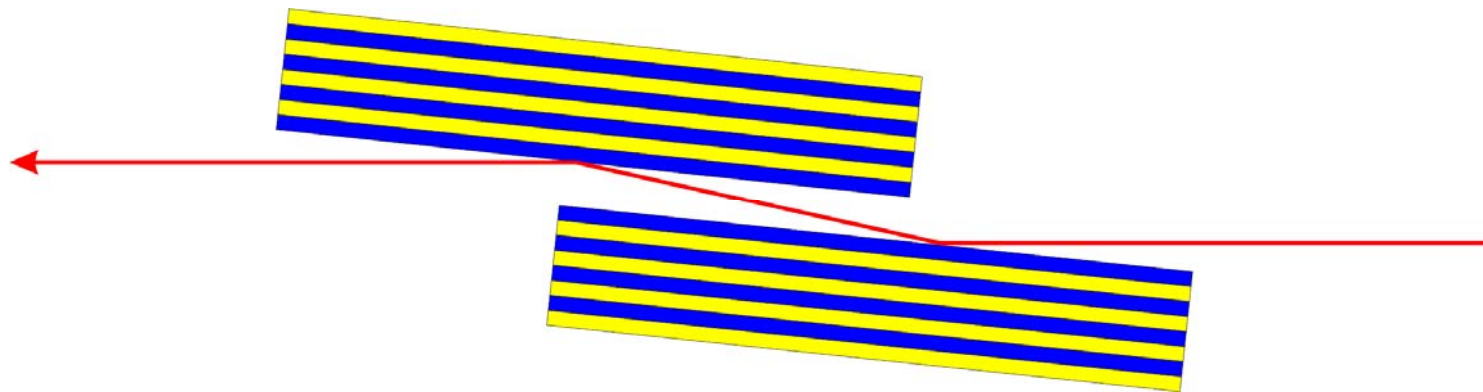


[19] T. Feigl et al, Jpn. J. Appl. Phys. 41, 4082 (2002)

Applications

Synchrotron optics: Multilayer high flux monochromators

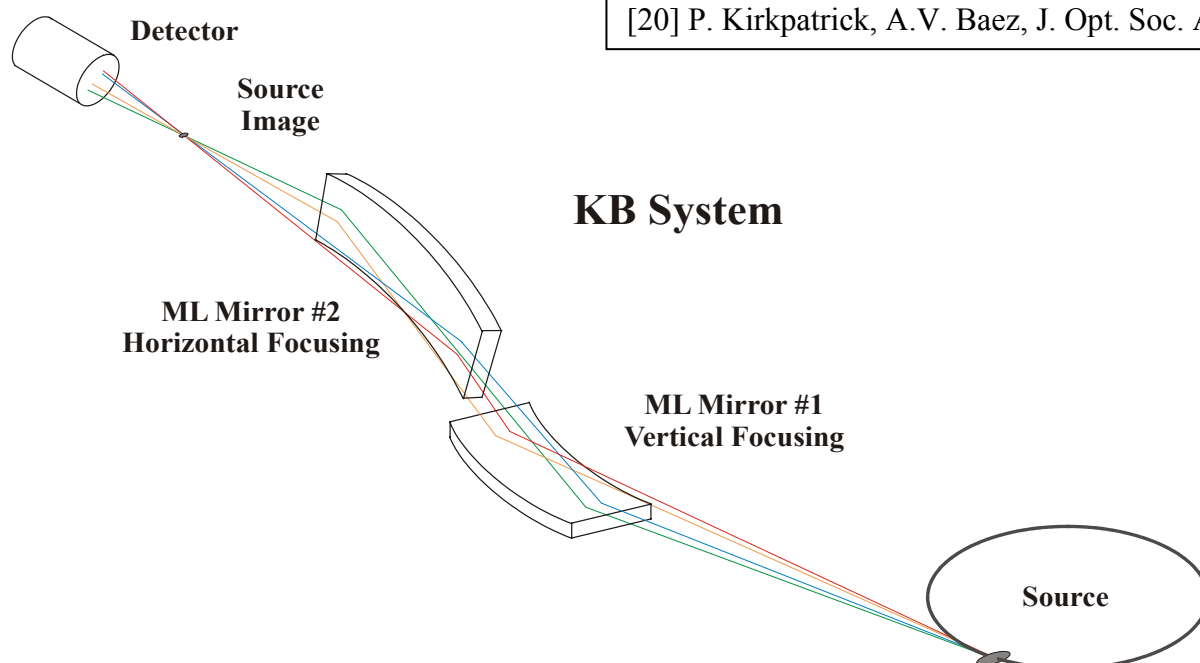
- Two bounce optics
- 100x larger bandwidth compared with Si(111)
- Harmonics suppression due to refraction and filling factor
- **Radiation and heat load issues !**



Applications

Synchrotron optics: Kirkpatrick-Baez (KB) focusing devices

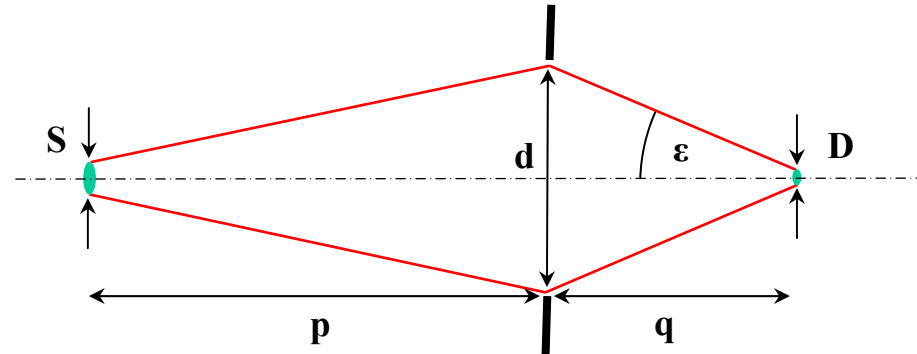
- Separate vertical and horizontal focusing (non-circular source)
- Technologically easier than single reflection ellipsoid + increased field of view
- Metal or graded ML coatings



[20] P. Kirkpatrick, A.V. Baez, J. Opt. Soc. Am. 38, 766 (1948)

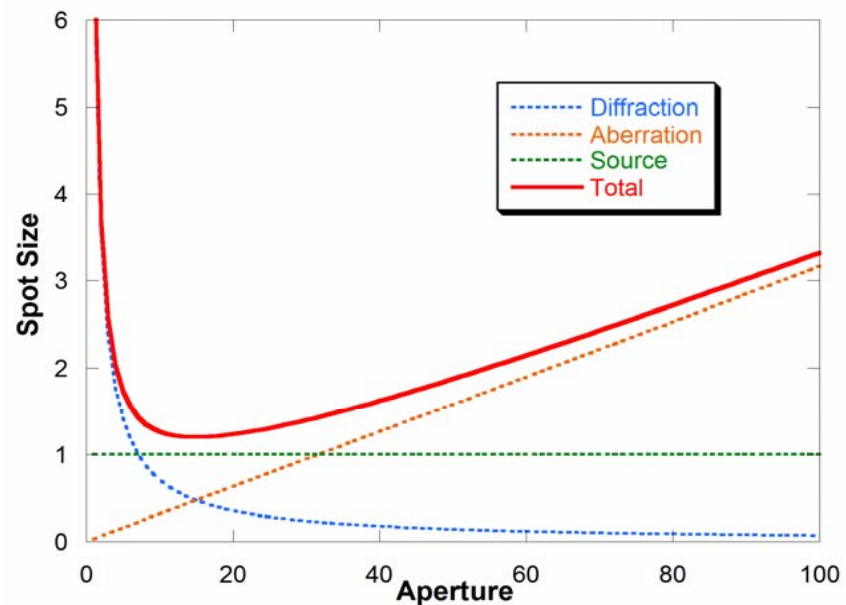
Applications - Limitations

Diffraction limit	$D_{FWHM} = C \frac{\lambda}{NA}$
Numerical aperture	$NA = n \cdot \sin \varepsilon$
Straight aperture	$C = 0.44$



Source size limit $D = \frac{q}{p} \cdot S$

- Further limitations**
- Volume diffraction
 - Scattering
 - Non-trivial design
 - Fabrication accuracy
 - Alignment



Applications

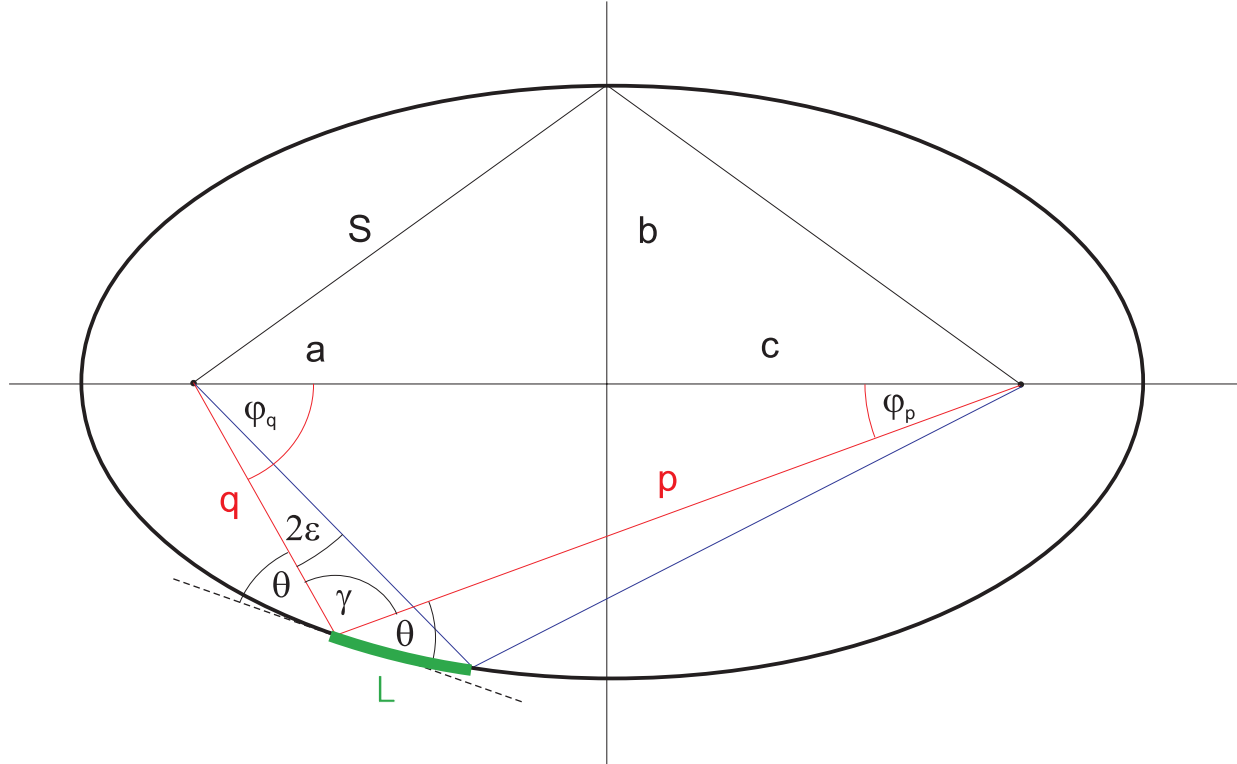
Ellipse geometry

$$2\varepsilon = \varphi_q(\theta_2) - \varphi_q(\theta_1)$$

$$\sin \varphi_q = \frac{p \cdot \sin 2\theta}{2 \cdot c}$$



$$NA = n \cdot \sin \varepsilon$$



Attention: Depth of aperture! → Wave front calculations

Applications

Simple approximation

Total reflection mirror

$$\sin \varepsilon \approx \frac{1}{4} \sin \theta_c = \frac{\sqrt{2 \cdot \delta}}{4} = \frac{\lambda}{4} \sqrt{\frac{r_0 \rho_e}{\pi}}$$

$$\Rightarrow D_{FWHM} \approx 1.76 \cdot \sqrt{\frac{\pi}{r_0 \rho_e}}$$

D_{FWHM} ≈ 25nm (Pt)

Multilayer mirror

$$\sin \varepsilon = \frac{1}{4 \cdot c} (p_2 \cdot \sin 2\theta_2 - p_1 \cdot \sin 2\theta_1)$$

$$\sin 2\theta \approx 2 \cdot \sin \theta \approx \frac{\lambda}{\Lambda}, p \approx 2 \cdot c$$

$$\Rightarrow \sin \varepsilon \approx \frac{\lambda}{2} (1/\Lambda_2 - 1/\Lambda_1)$$

$$\Rightarrow D_{FWHM} \approx \frac{0.88}{1/\Lambda_2 - 1/\Lambda_1}$$

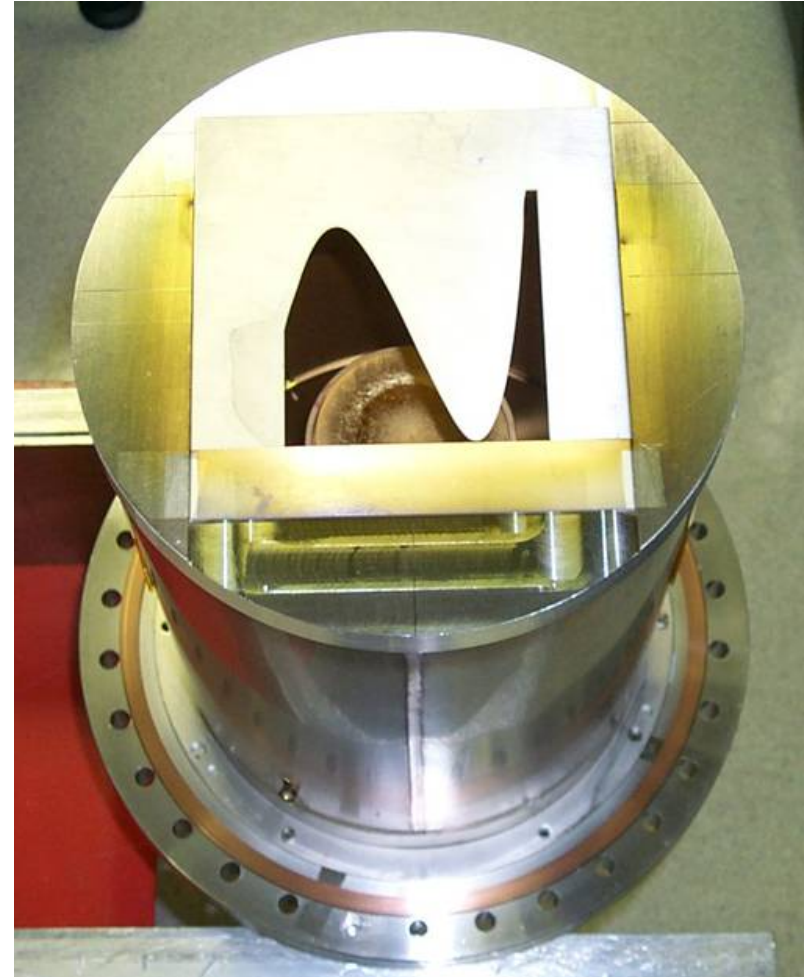
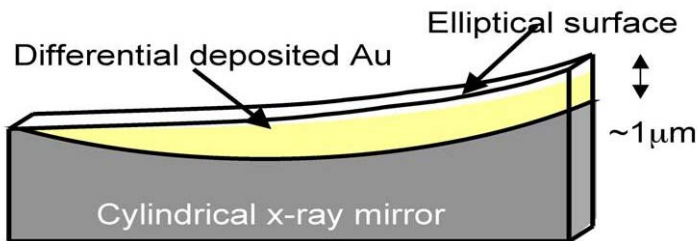
D_{FWHM} ≈ 5nm

No explicit energy dependence !

Applications

APS KB development

- Static total reflection mirrors
- Correct figure by thick Au coating
- Differential deposition along beam footprint
- Profile coating by masking along beam footprint

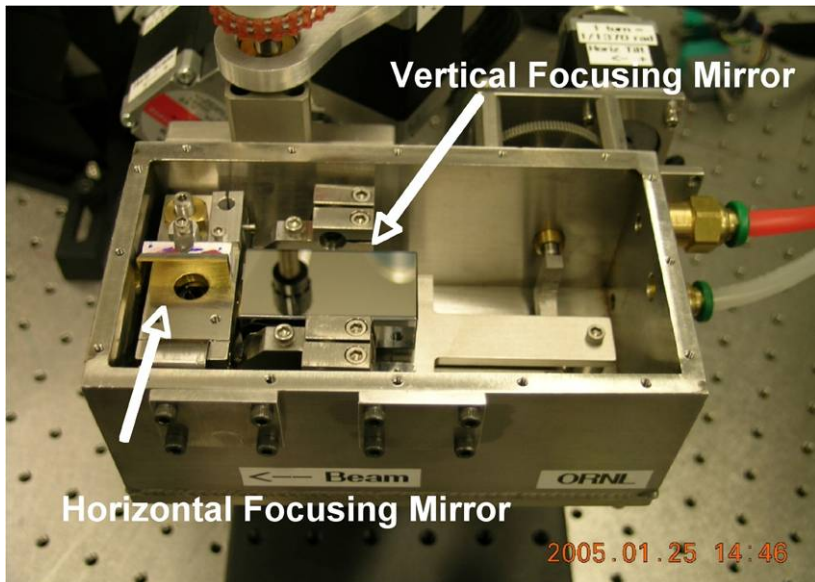


[21] G. Ice et al, Rev. Sci. 71, 2635 (2000)

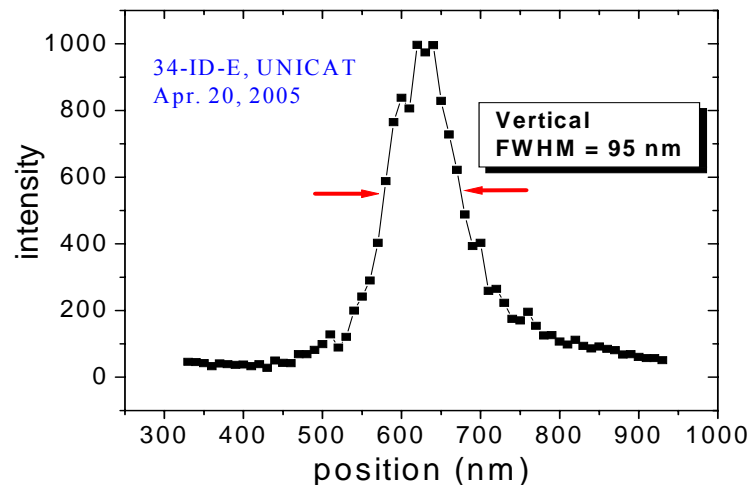
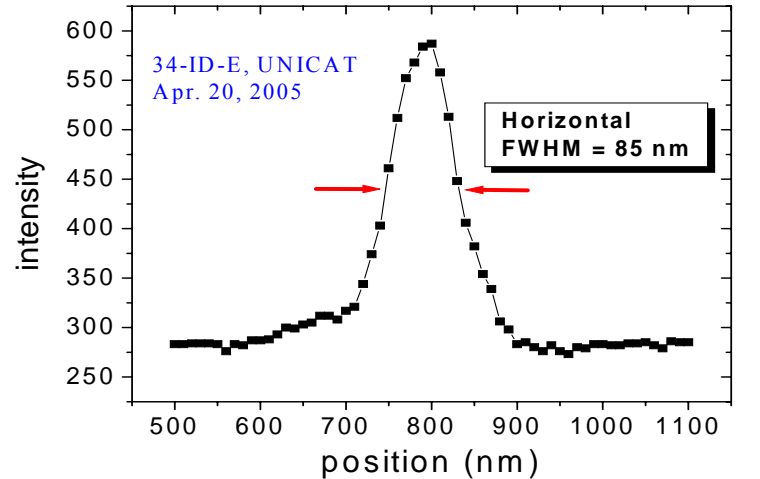
Applications

APS KB development

- White beam focusing experiment at sector 34
- Spot size below 100 nm



[22] C. Liu et al, Ref. Sci. Instr. 76, 113701 (2005)

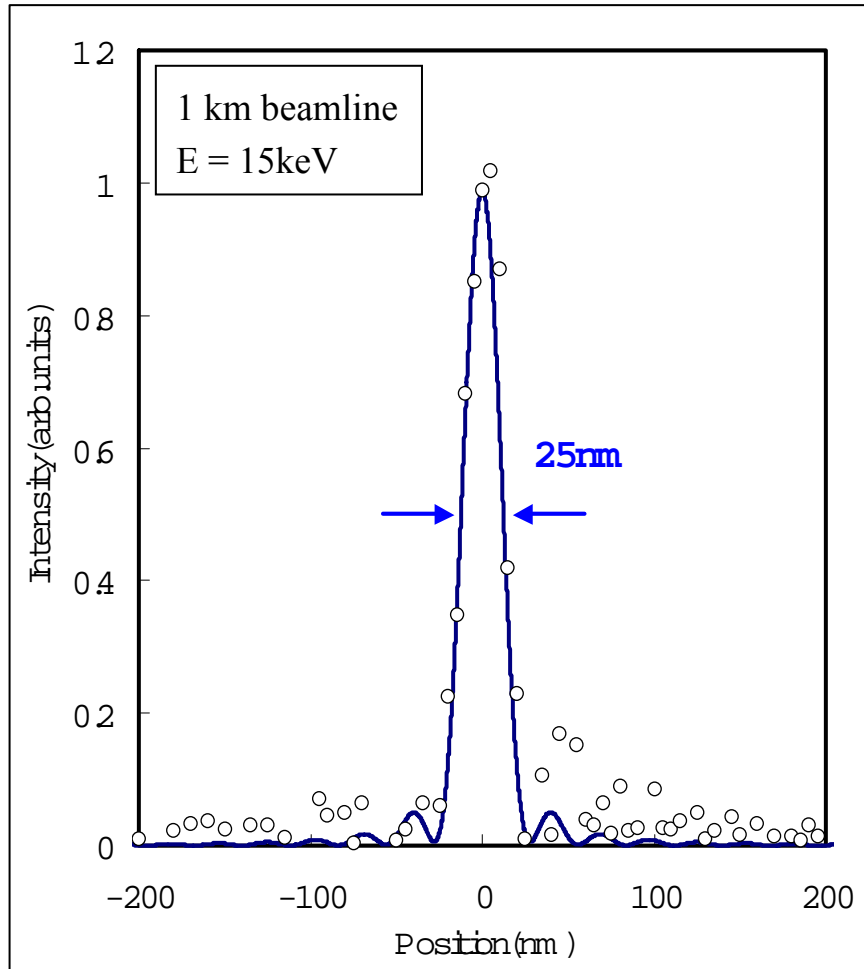


Applications

Spring-8/Osaka KB development

- Static and figured Si substrates
- Plasma Chemical Vapour Machining (PCVM)
- Elastic Emission Machining (EEM)
- Pt coating + thickness correction
- Focal spots below 30 nm
- Aiming less than 10 nm using multilayers

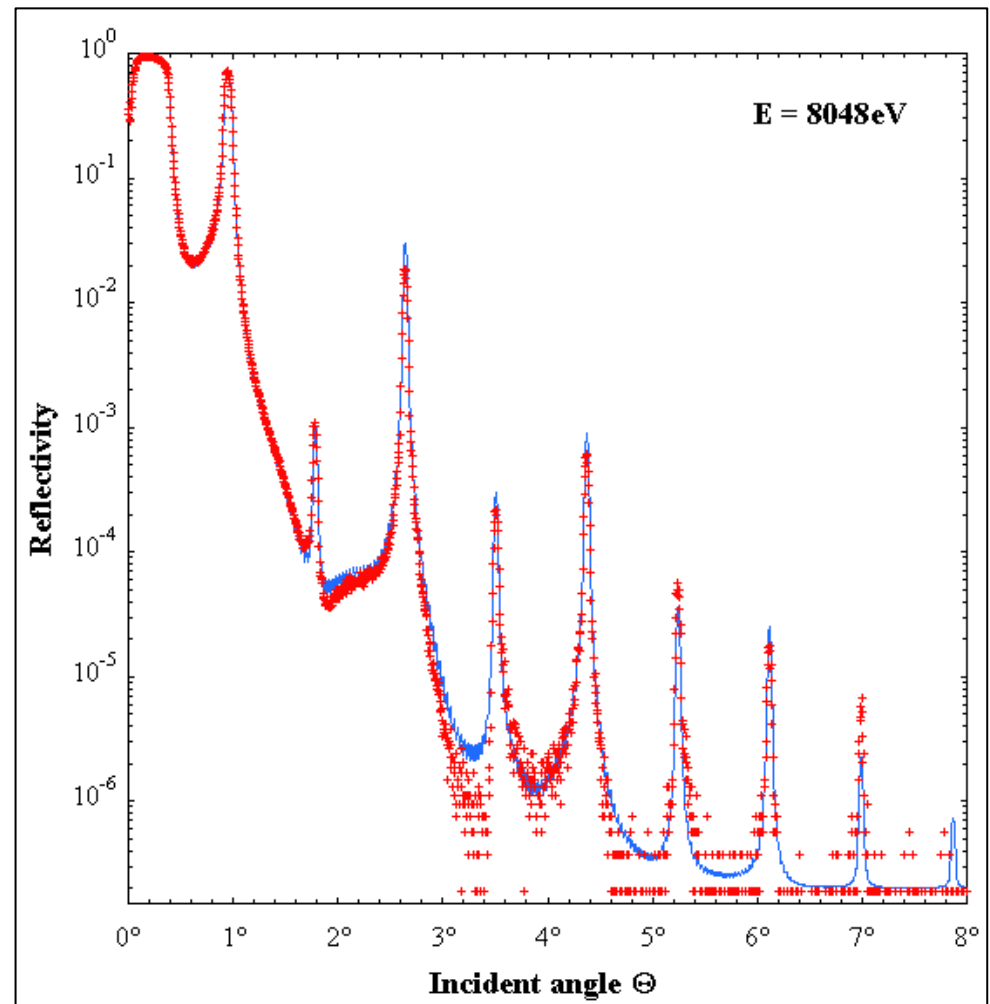
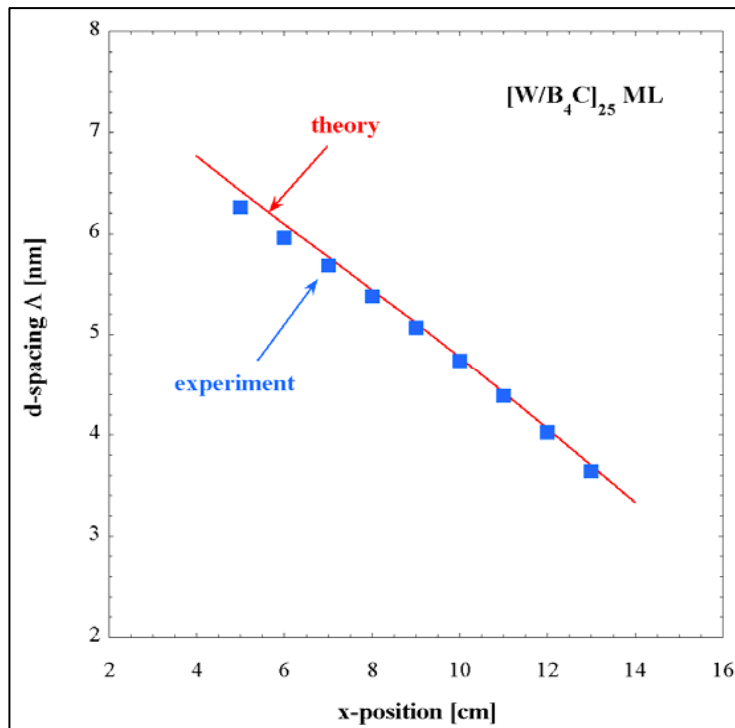
[23] H. Mimura et al,
Jpn. J. Appl. Phys. Part 2 44, 18539 (2005)



Applications

ESRF KB development

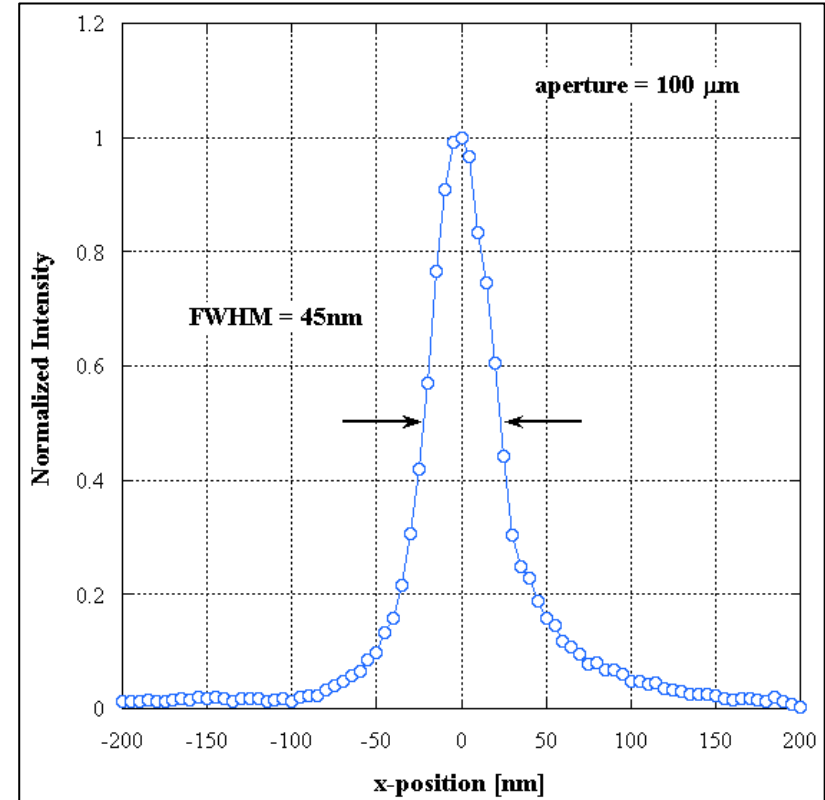
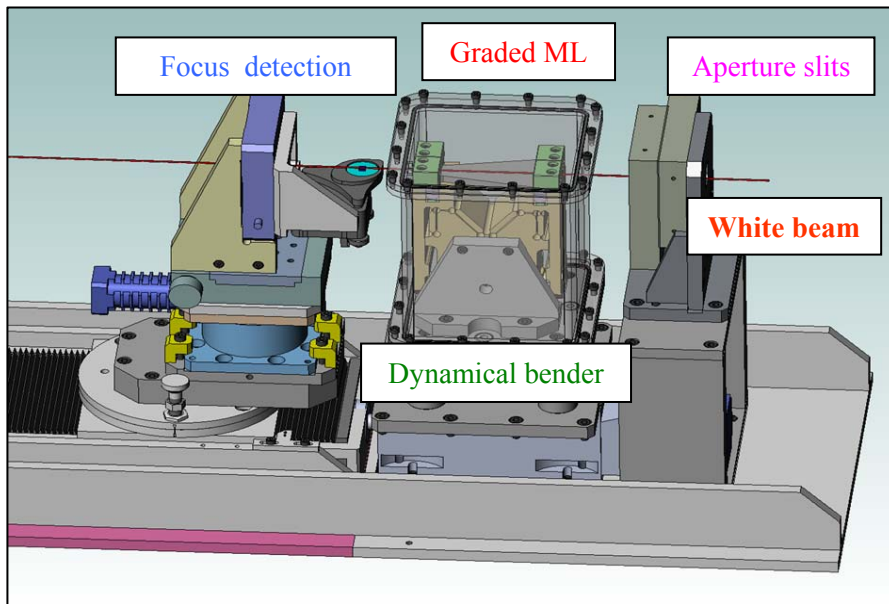
- Laterally graded multilayers
- Flat Si substrates



Applications

ESRF focusing experiment

- Full undulator spectrum
- Vertical line focus
- Dynamical bender
- Raw data **45 nm FWHM @ 100 μm aperture**

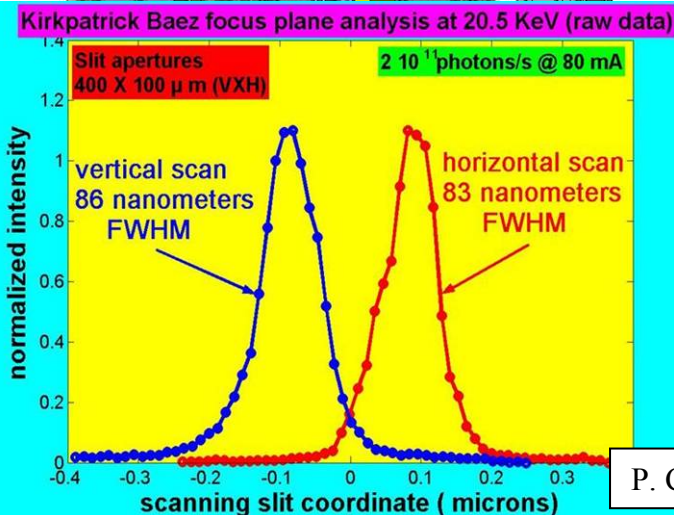
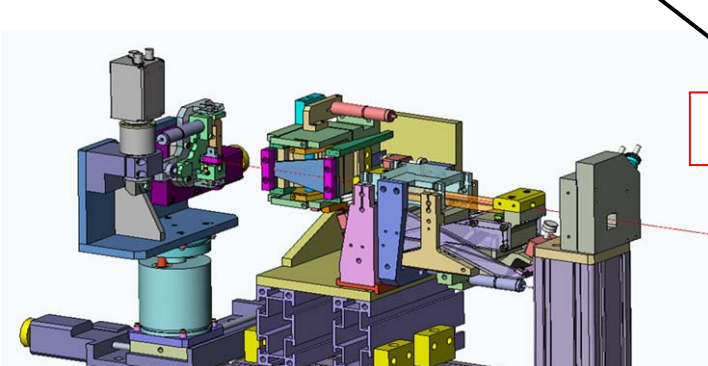


[24] Ch. Morawe et al, Proc. SPIE 6317 (2006)

Applications

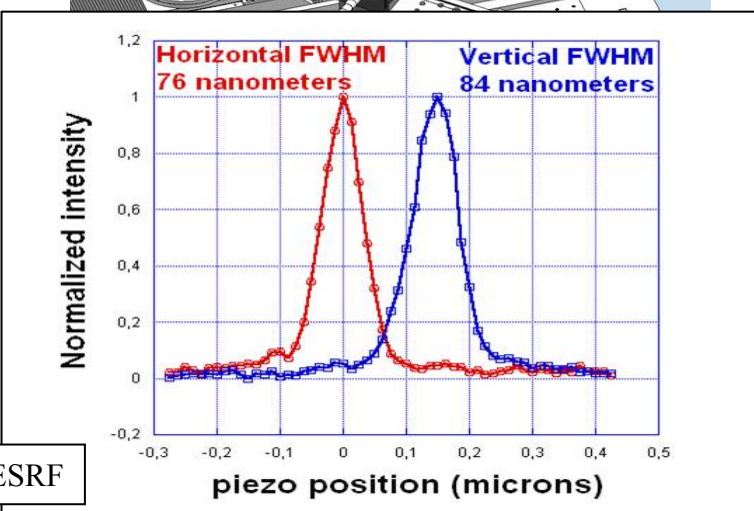
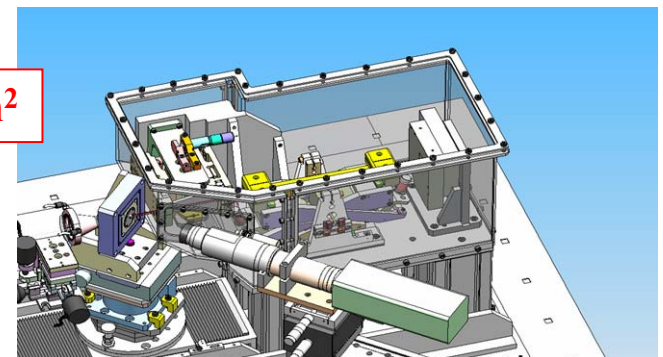
ID19: low β @ 150 m, E = 15...24 keV
 86*83 nm²: 2×10^{11} ph/s @ 80mA

3×10^5 ph/s/mA/nm²



P. Cloetens, O. Hignette, ESRF

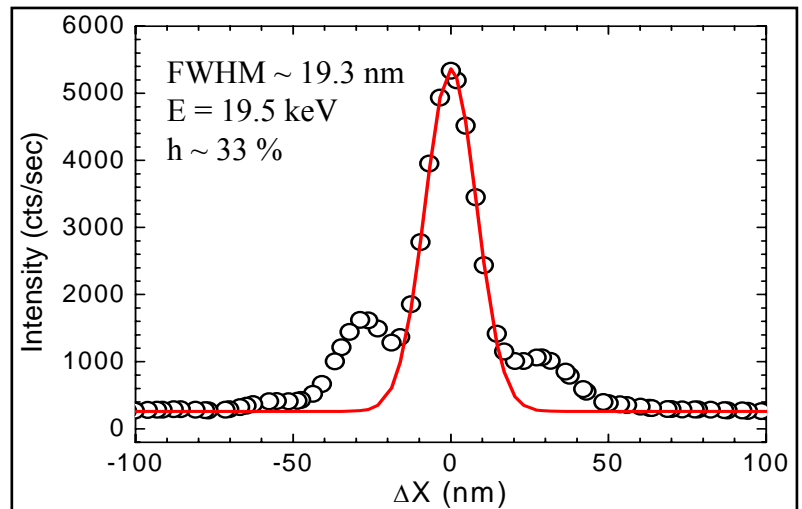
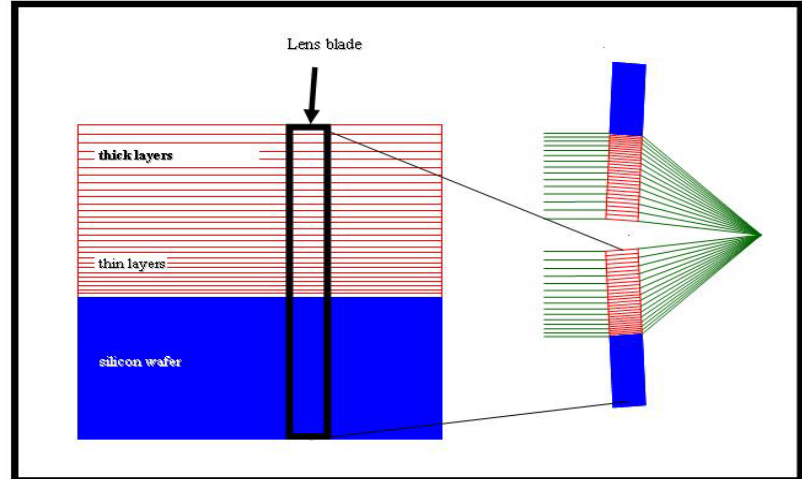
ID22: high β @ 60 m, slit source, E = 17 keV
 76*84 nm²: 10^9 ph/s @ 200mA
 150*100 nm²: 10^{12} ph/s @ 200mA



Applications

Multilayer Laue Lenses (APS)

- High aspect ration linear zone plate
- Transmission multilayer optics
- Bragg reflection to enhance efficiency
- Very thick depth graded coatings
- Starting with thinnest layer
- Crossed KB geometry possible
- Line focus **below 20 nm**



[25] H.C. Kang et al, Phys. Rev. Lett. 96, 127401 (2006)

Applications

Further mirror/multilayer based optics

- **X-ray astronomy (normal and grazing optics)**
- **Water window microscopy (Wolter)**
- **Plasma spectroscopy**
- **Laboratory X-ray instrumentation (commercial)**
- **Free Electron Lasers (FEL)**
- ...

Summary - Perspectives

Past achievements

- Theoretical treatment of flat multilayers well established
- Inclusion of experimental artifacts possible
- Tools for design and analysis available
- Advanced fabrication and characterization instrumentation
- Vast areas of application from visible light to hard X-rays

Areas of ongoing research and development

- Full wave optical treatment of curved multilayers
- Diffraction limited high aperture optics
- Improved understanding of radiation impact
- ...

References

1. J.H. Hubbel et al, *J. Phys. Chem. Ref. Data* **9**, 1023 (1980)
2. J. Als-Nielsen, D. McMorrow, “*Elements of Modern X-Ray Physics*”, Wiley, Chichester, UK (2001)
3. A. Thompson et al, “*X-ray Data Booklet*”, LBNL, University of California, Berkeley, USA (2001)
4. CXRO – ALS web site: <http://www-cxro.lbl.gov>
5. E. Spiller, “*Soft X-Ray Optics*”, SPIE Press, Washington, USA (1994)
6. A.G. Michette, “*Optical Systems for Soft X rays*”, Plenum Press, New York, USA (1986)
7. J.H. Underwood, T.W. Barbee Jr., *Appl. Opt.* **20**, 3027 (1980)
8. L.G. Parratt, *Phys. Rev.* **95**, 359 (1954)
9. K. Vestli, E. Ziegler, *Rev. Sci. Instr.* **67**, 3356 (1996)
10. P.H. Berning, *Physics of Thin Films*, J. Hass, ed. (Academic, New York, 1963)
11. M. Yamamoto, T. Namioka, *Appl. Opt.* **31**, 1622 (1992)
12. I.V. Kozhevnikov, I.N. Bukreeva, E. Ziegler , *Nucl. Instr. And Meth. A* **460**, 424 (2001)
13. Ch. Morawe, E. Ziegler, J-Ch. Peffen, I.V. Kozhevnikov, *Nucl. Instr. And Meth. A* **493**, 189 (2002)
14. Ch. Morawe, Ch. Borel, E. Ziegler, J-Ch. Peffen, *Proc SPIE* **5537**, 115 (2004)
15. J.A. Thornton, *Ann. Rev. Mater. Sci.* **7**, 239 (1977)
16. S. Bajit et al, *J. Appl. Phys.* **90**, 1017 (2001)
17. D.L Beke et al, *Vacuum* **50**, 373 (1998)
18. T. Tsuru, T. Harada, M. Yamamoto, *IPAP Conf. Series* **7**, 168 (2006)
19. T. Feigl et al, *Jpn. J. Appl. Phys.* **41**, 4082 (2002)
20. P. Kirkpatrick, A.V. Baez, *J. Opt. Soc. Am.* **38**, 766 (1948)
21. G. Ice et al, *Rev. Sci.* **71**, 2635 (2000)
22. C. Liu et al, *Ref. Sci. Instr.* **76**, 113701 (2005)
23. H. Mimura et al, *Jpn. J. Appl. Phys. Part 2* **44**, 18539 (2005)
24. Ch. Morawe et al, *Proc. SPIE* **6317** (2006)
25. H.C. Kang, J. Maser, G.B. Stephenson, C. Liu, R. Conley, A.T.Macrander, S. Vogt, *Phys. Rev. Lett.* **96**, 127401 (2006).

Thank you !